

RESTRICTED

NATIONAL ADVISORY COMMITTEE FOR AERONAUTICS



TECHNICAL NOTE

No. 951

TESTS ON THIN-WALLED CELLULOID CYLINDERS TO DETERMINE THE
INTERACTION CURVES UNDER COMBINED BENDING, TORSION,
AND COMPRESSION OR TENSION LOADS

By Elmer F. Bruhn
Purdue University



FOR REFERENCE

Washington
January 1945

NATIONAL ADVISORY COMMITTEE
FOR AERONAUTICS
LABORATORY

NOT TO BE TAKEN FROM THIS ROOM

CLASSIFIED DOCUMENT

This document contains classified information affecting the National Defense of the United States within the meaning of the Espionage Act, USC 50:31 and 32. Its transmission or the revelation of its contents in any manner to an unauthorized person is prohibited by law. Information so classified

may be imparted only to persons in the military and naval Services of the United States, appropriate civilian officers and employees of the Federal Government who have a legitimate interest therein, and to United States citizens of known loyalty and discretion who of necessity must be informed thereof.

RESTRICTED

RESTRICTED

NATIONAL ADVISORY COMMITTEE FOR AERONAUTICS

TECHNICAL NOTE NO. 951

TESTS ON THIN-WALLED CELLULOID CYLINDERS TO DETERMINE THE
INTERACTION CURVES UNDER COMBINED BENDING, TORSION,
AND COMPRESSION OR TENSION LOADS

By Elmer F. Bruhn

SUMMARY

The report on this research project is divided into two parts. Part I presents the results of preliminary tests to determine the modulus of elasticity of celluloid sheet; the effect of temperature change on the value of the modulus of elasticity; the creep of celluloid sheet under stress as a function of time; and finally the effect of repeated buckling failures on the original buckling strength of celluloid cylinders.

Part II of this report gives the results of tests on a considerable number of thin-walled, circular celluloid cylinders of several lengths, diameters, and wall thicknesses when subjected to loads producing pure compression, pure bending, pure torsion acting separately and in combination and of such magnitude as to cause failure of the cylinders.

Ultimate strength interaction equations based on the test results are given for circular cylinders subjected to combined compression and pure bending, combined compression and pure torsion, combined pure bending and pure torsion, and finally to combined compression, bending, and torsion.

Limited results are given for the celluloid cylinders subjected to combined tension and pure bending, combined tension and pure torsion, and finally to combined tension, bending, and torsion.

RESTRICTED

INTRODUCTION

The modern airplane body is essentially a thin-walled shell. In some body designs, all longitudinal skin stiffeners are removed or only three longitudinal skin stiffeners are used, thus the thin shell becomes the major structural unit in resisting the applied external loads. In general, the airplane body is subjected to external forces which will produce compressive, bending, and twisting stresses in the body structure.

Very little test information is available at present on the ultimate strength of thin-walled metal cylinders under combined loads, particularly so if compression, bending, and twisting loads are acting simultaneously. One reason for the lack of this information is due, no doubt, to the great cost and amount of time to carry out a complete test program on full-size metal cylinders. The purpose of this research project was to determine whether the testing of inexpensive small cylinders fabricated from thin celluloid sheet would give valuable reliable data for determining the ultimate strength interaction relationships for circular thin-walled cylinders when subjected to combinations of compressive, bending, and twisting loads.

It is thought that the results obtained in this project have shown definitely that valuable design information can be obtained from tests of celluloid cylinders with comparatively small expenditure of time and money.

The funds for this research project were supplied by the National Advisory Committee for Aeronautics. The project was carried out as a regular research project under the Purdue Research Foundation and the Purdue University Engineering Experiment Station.

The actual test work was carried on in the department of aeronautics of the School of Mechanical and Aeronautical Engineering under the direct supervision of Professor E. F. Bruhn. The test apparatus was constructed and the majority of the cylinder tests were made by Mr. R. L. Dickinson, former instructor of Aeronautical Engineering at Purdue University. The remainder of the tests were completed by Mr. W. G. Koerner, senior student at Purdue, and Professor Bruhn. The digest of the data and the writing of the report were carried out by Professor Bruhn.

The writer is indebted to Professor K. D. Wood for valuable suggestions and for reading the final report.

SYMBOLS

L cylinder length for minimum internal frame spacing, inches

D cylinder diameter, inches

r cylinder radius, inches

t cylinder wall thickness

R_c compression load ratio (non-dimensional)

$$\left(R_c = \frac{\text{applied compressive load on cylinder}}{\text{ultimate compressive load for cylinder}} \right)$$

R_b pure bending ratio (non-dimensional)

$$\left(R_b = \frac{\text{applied pure bending load on cylinder}}{\text{ultimate pure bending load for cylinder}} \right)$$

R_s pure torsion load ratio (non-dimensional)

$$\left(R_s = \frac{\text{applied pure torsion load on cylinder}}{\text{ultimate pure torsion load for cylinder}} \right)$$

$$R_c^x + R_b^y + R_s^z = 1.0$$

(an equation referred to as the ultimate strength interaction curve where the exponents x , y , and z define the general relationships of the load ratios when a cylinder is subjected to a combined loading which causes failure of the cylinder)

I - PRELIMINARY TESTS AND STUDIES

Summary

The primary object of the test project as a whole was to determine the ultimate allowable load interaction curves

for thin-walled cylinders when subjected to combined compressive, bending, and torsional loads. The material used for the test cylinders was the nitrocellulose compound commonly referred to as celluloid. It is common knowledge that for such plastic materials the stiffness of the material is influenced by temperature and also that the material suffers creep under stress. Preliminary tests were run to determine the extent of these factors.

The buckling of thin-walled cylinders falls in the general category of elastic buckling since the stresses that produce buckling are relatively low. Tests were run on cylinders to determine whether the ultimate buckling strength of cylinders was affected by repeated loading to buckling failure and also to determine the influence of time of loading upon the ultimate buckling strength.

Material

The material for all the test units in the test project was cut from standard 20- by 50-inch sheets of transparent celluloid, which were purchased from the Celluloid Corporation. Three nominal sheet thicknesses were used: namely, 0.0075 inch, 0.010 inch, and 0.015 inch.

Stress-Strain Diagrams of Celluloid Sheet

Figures 1 to 4 show the results of tests to determine a portion of the tension stress-strain curve for celluloid sheet material. The test specimens consisted of 12-inch strips varying from 0.125 to 0.25 inch in width, which were cut from the 20- by 50-inch celluloid sheets in directions parallel to the length of the sheet and also parallel to the width direction. A 10-inch gage length was carefully marked on the test strips. The test strips were held in position at one end by a rigid clamp placed to coincide with one of the gage marks and which was fastened to the table top. Tension loads were applied by means of a small flexible wire thread attached to the other end of the test strip, which in turn passed over a nearly frictionless pulley, with small weights being suspended on the end of the wire to load the test strip in tension.

The elongation of the 10-inch gage length was obtained by a "Carl Zeiss" measuring microscope set up over the gage mark near the free end of the test strip. Photograph No. 1

shows test setup for measuring the strain for the various tension loads. Strain readings were taken for two series of loadings. In the first series the strip load was added, the strain was read within 6 seconds and then the load was removed before adding the next larger load. Therefore, in this series the stress on the specimen existed for only a short interval of time. Curve A of figures 1 to 4 shows the results of this series of tests. In the second series of tests the loads on the test strips were applied continuously and not removed, and the loading was carried both up and down. To run a complete test on a strip required several minutes which meant that the test strip carried tensile stress for a considerable length of time. Curves B of figures 1 to 4 show the results of these tests.

Creep of Celluloid Sheet

Table 1 shows the results of tests to obtain information on the effect of stress intensity and time of stress duration upon the creep action of celluloid sheets. A test strip similar to that used for obtaining stress-strain curves was used in this test. The test strip was loaded with increasing tension loads and the strain in 10 inches was measured at various time intervals up to a maximum of 2 minutes. The results in table 1 are presented in graphical form in the curves below the table.

Effect of Temperature on Modulus of Elasticity

Figure 5 shows the effect of temperature change upon the stiffness in tension for celluloid sheet material. Thin strip specimens similar to those used for obtaining the test data for the stress-strain curves as previously discussed were cut from the 20- by 50-inch celluloid sheets. These strips were loaded in tension by a single load and the elongation in a 10-inch gage length was obtained by a measuring microscope. The modulus of elasticity was computed on the basis of this unit strain and the accompanying stress. Tests were run at room temperature varying between 65° and 95° F. The curves in figure 5 should not be considered as giving the correct value of E , since only one point on the stress-strain curve was obtained. The purpose of the tests was only to obtain a measure of the effect of temperature change upon the stiffness of the celluloid sheet in tension.

General Conclusions from Stress-Strain, Creep,
and Temperature Tests

The following general conclusions can be drawn from a study of the results (figs. 1 to 5 and table 1):

1. The modulus of elasticity in tension for the 20- by 50-inch celluloid sheets is not the same for stresses parallel to the length and width of the sheets. The difference, however, is usually less than 10 percent. (See fig. 5.)

2. There is considerable variation in the value of the modulus of elasticity with sheet thickness. The thinner the sheet the higher the stiffness. The variation for sheets of 0.0075-inch and 0.015-inch thickness is around 20 percent.

3. Over the range of stress used in the stress-strain tests, the resulting curve is practically straight. Reference to the buckling stress for test cylinders in the latter portion of this report will show that the maximum stress at buckling was around 300 to 400 psi, which stress range falls on the lower portion of the stress-strain data of figures 1 to 4, where the relationship between stress and strain is definitely a straight line. It is assumed that the compressive stress-strain relation at low compressive stresses is the same as for tension stresses. The buckling of the cylinders should therefore fall in the elastic category if the influence of creep is eliminated.

4. An increase in temperature decreases the stiffness of the celluloid sheet material. For example, for a sheet 0.010 inch in thickness, the stiffness changed from approximately 450,000 psi to 400,000 psi when the temperature was changed from 65° to 95° F. (See fig. 5.)

5. Celluloid sheet under stress suffers the characteristic generally referred to as creep. Table 1 shows, however, if the stresses are kept under 500 psi and the time interval of stress application within 0.25 of a minute, the unit strain due to creep is negligible.

These preliminary tests on stress-strain properties therefore definitely indicated that if reliable and consistent comparative results were to be obtained in testing celluloid cylinders under combined stresses, the tests on any cylinder should be run at the same temperature and that the time interval used in applying the loads should be short and that it should be kept nearly the same in order to eliminate the

influence of temperature and creep on the buckling strength of cylinders fabricated from thin celluloid sheet.

Preliminary Tests to Determine Effect of Repeated Failure
and Effect of Time of Loading on Cylinder Strength

Two preliminary test cylinders were fabricated. They will be referred to as cylinders P-1 and P-2. Cylinder P-1 was 6.87 inches in diameter, 7 inches long, and had a wall thickness of 0.0075 inch. Cylinder P-2 was the same as cylinder P-1 except the length was 28 inches. The method of fabrication of these two cylinders was similar to that of the cylinders in part II of this test program, which is described in detail in part II.

These two test cylinders were loaded in pure bending and pure torsion by means of a system of levers, wire thread, and nearly frictionless pulleys. (See fig. 6 for schematic diagram of the loading system.) (See photos. Nos. 2 to 9 for pictures of these cylinders.)

Table 2 gives the results of the pure bending and torsion tests on test cylinder P-1. Nine tests each were made in bending and torsion and the load which caused buckling failure each time was read on the platform scale. As shown in table 2, the time interval required to produce buckling failure was varied between 0.10 to 0.93 minute for the pure bending tests. The scale loads to cause failure for the first and ninth tests were 3 pounds 8.3 ounces and 3 pounds 8.4 ounces, respectively, with time of loading 0.10 and 0.13 minute, respectively. Thus, after the cylinder had failed by buckling eight times, the ninth time gave a failing strength practically the same as the first loading when the time of loading was kept practically the same. When the time of loading was increased to 0.93 minute (see table 2), the scale load which caused failure dropped to 3 pounds 6.5 ounces, or a decrease of 3.3 percent from the strength in test No. 1 where time of loading was 0.13 minute.

Table 2 also gives the results of nine tests in pure torsion. The percent difference between the strength of the cylinder in the first and ninth tests was 0.66 and the maximum variation from the average strength of nine tests was 2.2 percent.

Tables 3, 4, 5, and 6 give the results of repeated failure tests on test cylinder P-2 in pure torsion and pure bending. The cylinder in table 3 was 28 inches long. For the tests in tables 4, 5, and 6, intermediate bulkheads were added to the original cylinder, thus giving cylinders with L/D ratios from 1 to 4. The time of loading to cause failure was varied. As indicated by the results in these tables, the maximum variation in strength under repeated loadings was not large.

Failure of all the test cylinders was sudden. At the first evidence of buckling the scale reading dropped off, and as the buckles spread and increased in depth the scale reading decreased. Thus it was necessary only to watch the pointer on the balance scale to obtain the buckling strength. The buckling was not explosive in character but progressed from a small buckle to large buckles in a fraction of a second. This type of failure also was true for all the combined load tests for the test cylinders in part II.

General Conclusions from Tests of Preliminary

Cylinders P-1 and P-2

The results in tables 2 to 6 indicated that the buckling strength of thin-walled celluloid cylinders in pure bending and pure torsion remained practically the same under repeated failure tests, if the time of loading was kept the same. This fact would tend to indicate that reliable comparative results could be obtained for the shape of the interaction curves, under combined loadings, since a single test cylinder could be loaded to failure many times without affecting its original failing strength.

Since temperature change affects the elastic properties of celluloid sheet the tests on any one cylinder should all be run with the same room temperature.

II - TESTS ON CYLINDERS UNDER COMBINED LOADS

Summary

Part II of this report presents the results of more than a thousand individual tests on 29 variations of test cylinders when subjected to combined loads involving compression,

tension, pure bending, and pure torsion. Equations for ultimate strength interaction curves based on the test results are presented.

Test Specimens

All test cylinders were fabricated from standard 20- by 50-inch sheet colluloid which was purchased from the Celluloid Corporation. Three sheet thicknesses were used, the nominal thickness being 0.0075 inch, 0.010 inch, and 0.015 inch. A few cylinders using a sheet of 0.0050-inch thickness were made but perfect cylinders without local buckling could not be obtained with this thickness and thus the 0.0050-inch sheet thickness was not used for any cylinder load tests.

The following table gives information regarding the variation of the thickness of the sheet units which made up the test cylinders. As indicated, the variation was considerable. This fact is not considered serious, since the preliminary tests in part I showed that a celluloid cylinder could be repeatedly loaded to failure with very little change in the ultimate buckling load; thus if the same cylinder is used for a complete series of tests, the variation of sheet thickness is common to all tests and thus its influence on the results should not be of appreciable importance.

Variation in Sheet Thickness

Nominal thickness	Measured thicknesses along circumference of test cylinder	Variation (percent)
0.015	0.0170, 0.0167, 0.0164, 0.0163, 0.0161, 0.016, 0.0159, 0.016, 0.016	6.9
0.010	0.0102, 0.010, 0.010, 0.0098, 0.0097, 0.0095, 0.0094, 0.0095,	7.3
0.0075	0.0073, 0.0072, 0.0072, 0.0073, 0.0074, 0.0075, 0.0076, 0.0075	5.5

Table 7 gives a summary of geometrical data on the cylinders which were tested. Sixteen individual test cylinders were fabricated. These cylinders were modified to give the 29 test cylinders in column (2) of table 7. For example, cylinders originally were fabricated with lengths of approximately 7, 10, and 14 inches in length. After these lengths were carried through a complete series of tests, the length

of the cylinder was changed either by cutting a portion off the cylinder or by inserting intermediate bulkheads between the end bulkheads of the test cylinder, which would thus change the L/D ratio for the cylinder.

Two cylinder diameters were used: namely, 7 inches and 12 inches, approximately. The lengths of the 7-inch diameter cylinders varied from 14 inches down to 3.5 inches and the 12-inch diameter cylinders from 6 inches to 12 inches in length. Three sheet thicknesses were used: namely, 0.0075 inch, 0.010 inch, and 0.015 inch. The r/t (radius/thickness) value of the test cylinders therefore varied from 230 to 800.

Fabrication of Test Cylinders

The lengths of the 6.88-inch diameter cylinders were 13.8 inches, 10.15 inches, 6.85 inches, and 3.40 inches. For the 12-inch diameter cylinders two lengths: namely, 6 inches and 12 inches, were fabricated. For the shorter lengths of the 6.88-inch diameter cylinders a circular wood form block was found satisfactory for forming the cylinders. Sheets 21.7 inches in length which allowed 0.1 inch for overlap were wrapped around the form block and held in place with a cloth tape. A permanent joint at the overlap was made with amyl acetate, which is a solvent for celluloid. This fluid was run in between the overlapping sheet edges by capillary action. In several minutes' time the sheets were securely joined together and the cloth tape could be removed and the cylinder removed from the form block for insertion of the end bulkheads.

For the longer cylinders, difficulty was encountered in making a perfect circular wood form block, and thus the longer cylinders of 6.88-inch diameter and all the 12-inch diameter cylinders were fabricated as follows:

The sheet was cut accurately to the required length plus 0.1 inch for overlap. One edge of the sheet was clamped to a square wooden bar, leaving about $1/4$ inch protruding out from the face of the clamp and resting on the face of the square bar. The other end of the sheet was brought around under the square bar and slipped under the sheet edge protruding from the clamp. Resistance of the clamped free edge of the sheet to bending provided the force necessary to keep the other free edge in contact with the clamped free edge. The 0.1-inch overlap of the sheets was welded together by inserting amyl acetate by capillary action. The forms and apparatus

for fabricating the cylinders are shown in photographs Nos. 10 and 12.

The cylinders were held in a circular shape by the insertion of a circular bulkhead at each end. The end bulkheads were made from 3-ply plywood $1/4$ inch in thickness and were turned out to the exact required diameter on a lathe. The cylinders were mounted in the test jig as cantilever beams; thus one end bulkhead was fastened rigidly to the test jig. The test loads were applied to the other end bulkhead. For applying bending and torsional couples a wood arm 35 inches in length was glued to the end bulkhead in the free end of the test cylinder. The bulkheads were fastened to the cylinder walls by use of amyl acetate, which provided a bond between the sheet and bulkhead which did not rupture under the cylinder test stresses.

For some of the test cylinders intermediate bulkheads were inserted. These bulkheads were turned to accurate dimensions from $3/32$ inch to 3-ply mahogany plywood. These bulkheads were likewise fastened to the cylinder walls by the amyl acetate. (See photo. No. 11.)

In general, the shorter cylinders were made by removing the end bulkhead at the free end and cutting the cylinder down to the desired length. This was possible because the repeated failure tests, the results of which are recorded in part I of this report, showed that buckling failure did not change the strength of the cylinder appreciably.

Description of Test Apparatus

All cylinders were tested with one end rigidly fastened to the test jig and all loads were applied to the other end of the cylinder. In building a supporting jig, it was important to obtain a rigid structure and yet have one in which the operator of the tests would have free access to the mounted cylinders and the wire-pulley-lever systems for applying the loads. Therefore the test jig consisted of four vertical corner members made from $2\frac{1}{2}$ - by $2\frac{1}{2}$ - by $1/4$ -inch angle irons. These four corner members were bolted together by transverse angle irons near the top and also at a point about 18 inches above the bottom ends of the uprights. The structure consisted, therefore, of four rectangular panels without diagonal shear bracing in order to permit accessibility to test cylinder and loading apparatus from all sides. Since the test loads on the cylinder were exceedingly small

compared to the cantilever strength of the heavy corner members of the test jig, the jig supporting structure could be classed as a rigid structure.

One end bulkhead of the test cylinders was bolted to a heavy wood block, which in turn was bolted to steel angle irons attached to the upper transverse jig structural members. The lower transverse angle irons supported a $1\frac{1}{2}$ -inch thick wood floor which provided the support for the speed reducers and the scales for measuring the reactions from the lever system which was used to apply the loads to the cylinders.

Figure 7 shows a diagrammatic sketch of the test jig. Photograph Nos. 17 to 20 show various views of the test jig.

Apparatus for Applying Pure Bending and Pure Torsional Loads

Figure 8 shows a schematic diagram of the bending and torsion apparatus. Pure bending and pure torsion were applied by a single speed reducer. This unit, hand cranked, pulls down on lever (A), one end of which rests on a platform scale. The other end is connected through a movable pivot to a second lever (B), on either end of which is a frictionless pulley.

For the torsion apparatus a wire is attached to one end of the lever (C) on the bottom bulkhead of the test cylinder. The wire is drawn horizontally at right angles to the lever, across a pulley mounted on the test jig structure, down and around the pulley on the end of lever (B). It is then brought to the back of the test jig around two more pulleys, past the back end of lever (C) and around the last pulley, where it reverses its direction and returns to be attached to the other end of lever (C). Thus, a pull-down on lever (B) will apply a pure torsion couple to the test cylinder.

For the pure bending apparatus (see fig. 8) a second wire is attached to the near end of lever (C). This wire is brought down around the second pulley on lever (B), then passes up and across the top of the jig to the other side, then down and fastens to the other end of lever (C). Thus, a down-pull on lever (B) also applied a pure bending load to the test cylinder.

Apparatus for Applying Axial Compression

The axial compression load on the test cylinders was applied through an entirely separate lever system. Figure 9 shows a schematic diagram of the system for applying the compression load to the test cylinders. A scale, a speed reducer, and three levers were used. The first lever (A) is supported at one end on the platform scale, the other end rests in a connecting pivot to the end of the second lever (B). The other end of lever (B) was supported on the rigid test jig frame. Lever (B) is attached to one end of lever (C) by a flexible wire. Lever (C) is pivoted at a short distance from the other end from which a wire is dropped through a hole in the upper platform of the test jig to attach by a hook to the midpoint of the lower cylinder bulkhead. Thus a down pull on lever (A) will apply a pure compression load to the test cylinder.

Influence of Friction in Loading System

Although so-called "frictionless" pulleys were used to support and guide the five wires by which bending and torsional couples were transmitted, a check was made on the amount of friction in the wire-pulley loading system. Tests made on each loading system: namely, bending, torsion, and compression, showed that the friction loss remained directly proportional to the magnitude of the applied loads. Thus the friction factor was constant regardless of load. Since the test data as illustrated in the appendix is in the form of load ratios in order to plot interaction curves, the friction factor cancels out and hence may be disregarded in plotting load interaction curves. If the true cylinder forces are wanted in order to calculate stresses, the friction factor must be considered as explained in the appendix.

General Test Procedure

To obtain test data for plotting ultimate strength interaction curves under combined compression, bending, and torsion loads, it is necessary to determine the ultimate strength of the cylinder under each of the three types of loading acting separately as well as under various combinations of the three types of loading.

The test results as given in part I of this report showed that if cylinder tests were run at the same room temperature and the time of loading was kept within 10 to 20 seconds,

consistent results could be obtained in the repeated ultimate buckling strength of celluloid cylinders. Therefore in making a series of tests on a cylinder, special effort was made to keep the rate of loading approximately the same with the time of test around 10 to 15 seconds.

For any given test cylinder, the general steps in the test sequence were approximately as follows:

1. Pure bending test
2. Pure torsion test
3. A series of five tests in combined bending and torsion with different proportions of bending and torsional loads
4. Check tests of pure bending and pure torsional strength
5. Pure compression test
6. A series of tests in combined torsion and compression using controlled values of compression - for example, 0.2, 0.4, 0.6, and 0.8 of the ultimate compressive buckling strength
7. A series of tests in combined bending and compression using controlled values of compression - for example, 0.2, 0.4, 0.6, and 0.8 of the ultimate compressive buckling strength
8. A series of tests for combined compression, bending and torsion using controlled values of compression equal to 0.2, 0.4, 0.6, and 0.8 of the ultimate compressive strength
9. On several of the test cylinders a series of tests for combined tension, bending, and torsion were run. Controlled values of tension based on the ultimate compressive strength were used, the tension being regarded as negative compression.
10. On a number of test cylinders, the pure bending force was replaced by cantilever bending due to a transverse load and a series of combined loading tests were run as described above.

Step 1 involved the application of a bending couple only to the test cylinder and increasing the magnitude of the couple until the cylinder failed by buckling on the compression side. The tare and gross scale readings were recorded, together with the lengths of the lever arms and the room temperature.

The procedure in step 2 was similar, with a torsion couple being applied until the cylinder failed by buckling on diagonal lines around the cylinder. As before, the scale readings and lever arm lengths were recorded.

In step 3 bending and torsional couples were applied simultaneously.

Step 4 provided a check on the maximum bending and torsional strength. This step was repeated after approximately every eight individual tests to provide a continuous check on the cylinder strength as compared to its original strength.

Step 5 involved the applying of a pure compression load to the cylinder until the cylinder failed by buckling. The scale readings and lever arms were recorded.

Step 6 was similar to step 3, with bending replaced by compression in order to obtain data for the interaction curve in combined torsion and compression.

Step 7 was the same as step 6 with bending replacing torsion. These results gave data for plotting the interaction curve in combined compression and bending.

Step 8 consisted of a number of tests in which bending and torsional couples as well as compressive loads were applied to the cylinder until it failed by buckling. In these tests the compression load was kept constant, while the couples were increased in magnitude until failure occurred.

Photographs Nos. 21 to 33 illustrate the buckling patterns of the cylinders under the various types of loading.

Test Data

All the cylinder test data are recorded in the form of graphs, which are included in this report. To illustrate the form of the test data, two tables of test data for two test cylinders are presented in the appendix. The explanation of the test terms also are given there.

Results and Discussion

Results of Tests for Cylinders in Combined Compression and Pure Bending

Figure 10 shows a plot of the load ratio R_c against

the load ratio R_b as obtained from the various cylinder tests. The values for the plotted points are taken from the tables in the appendix. The test values in figure 10 are plotted without distinction of r/t or L/D of the cylinders. The results show that the majority of the test results lie above the straight line relationship as given by the equation $R_c + R_b = 1$. A mean curve through the test results is given closely by the equation $R_c + R_b^{1.1} = 1$, which is plotted on figure 10.

Figure 11 shows a plot of the test data for the cylinders divided into three groups, each having a different L/D (length/diameter) ratio. For the two cylinder groups with L/D near 1.0 and 1.5 to 2.0, respectively, the interaction equation $R_c + R_b^{1.1} = 1$ represents mean results. For the cylinder group for $L/D = 0.5$ to 0.67, the mean of the test results appears to fall between a straight line and the equation $R_c + R_b^{1.1} = 1$. Thus the general conclusion is drawn that the lower limit of the test results is closely approximated by the interaction equation $R_c + R_b = 1$ and the mean results by the equation $R_c + R_b^{1.1} = 1$.

The r/t (radius/thickness) ratio for the cylinders which varied from 230 to 800 appears to have no influence on the load ratio R_c and R_b . (See fig. 11.)

Results in Combined Compression and Pure Torsion

Figure 12 shows a plot of the load ratio R_c against the load ratio R_s as obtained for all cylinder tests. The test values in figure 12 are plotted without distinction of r/t or L/D of the cylinders. In figure 12 the mean of the test data is approximated closely by equations $R_c + R_s^{2.5} = 1$ and $R_c^{1.1} + R_s^{2.5} = 1$, the first equation checking closer at high values of R_s and the other equation checking better at lower values of R_s . The lower limit of all the test data is closely approximated by the equation $R_c + R_s^2 = 1$, which is plotted on figure 12.

Figure 13 shows a plot of the test data for the cylinders divided into three groups of different L/D ratio. The curve for the interaction equations, $R_c + R_s^2 = 1$,

$R_c^{1.1} + R_s^{2.5} = 1$ and also $R_c + R_s^3 = 1$ are plotted on these figures. The results show that for the long cylinder group all the test values fell on or outside the curve for the equation $R_c^{1.1} + R_s^{2.5} = 1$. For the cylinder group with L/D around 1.0 the equation $R_c^{1.1} + R_b^{2.5} = 1$ approximates the mean results closely. For the short cylinder group ($L/D = 0.5$) the curve for the equation $R_c^{1.1} + R_s^{2.5} = 1$ is slightly above the mean results for high values of R_s and the curve $R_c + R_s^{2.5} = 1$ would be a better approximation in this region. (See fig. 12.)

Results, Combined Pure Bending and Pure Torsion

Figure 14 shows a plot of the load ratio R_b against the load ratio R_s as obtained for all the cylinder tests. The test values in figure 14 are plotted without distinction of r/t or L/D for the cylinders.

The mean of the test data is closely approximated by either of the equations, $R_b^{1.21} + R_s^{2.5} = 1$ or $R_b^{1.5} + R_s^2 = 1$ as shown on figure 14. For large values of the load ratio R_s the equation $R_b^{1.5} + R_s^2 = 1$ is a better mean approximation with the reverse being true for region of low values of R_s . The lower limit of all the test results is given by the equation $R_b + R_s^2 = 1$ and the upper limit of the test data is fairly well represented by the equation $R_b^2 + R_s^2 = 1$.

Figure 15 shows a plot of the test data for the cylinders divided into three groups of different L/D ratio. The curves for the equations $R_b + R_s^2 = 1$, $R_b^{1.21} + R_s^{2.5} = 1$, and $R_b^2 + R_s^2 = 1$ are plotted on this figure. The curve for equation $R_b^{1.5} + R_s^2 = 1$ is not plotted in order to avoid confusion of too many curves on a small drawing. For the cylinder group with L/D of 0.5 to 0.67 the mean test data is closely approximated by the curve $R_b^{1.21} + R_s^{2.5} = 1$. For the cylinder group with $L/D = 1.0$, the curve from equation $R_b^{1.5} + R_s^2 = 1$ would fall closer to the mean results

for test data in the range of $R_b = 0$ to 0.4 . For the cylinder group with $L/D = 1.5$ to 2.0 , all test results fell near the curve as given by the equation $R_b^2 + R_s^2 = 1$.

Results, Combined Compression, Pure Bending, and Pure Torsion

Figures 16, 17, and 18 show a plot of the test results for the various test cylinders when loaded in combined compression, bending, and torsion. In running the tests the load ratio R_c in compression was kept constant for a series of tests. In general, the constant values of R_c used were 0.2 , 0.4 , 0.6 , and 0.8 .

Figure 19 shows a composite plotting of all test cylinders for the four series of tests with R_c kept constant and equal to the values shown. The curves for three interaction equations are plotted on each of the four graphs: namely, $R_c + R_b + R_s^2 = 1$, $R_c + R_b + R_s^{2.5} = 1$, and $(R_c + R_b^{1.1})^{1.1} + R_s^{2.5} = 1$. The lower range of the test data is closely approximated by the curve for the equation $R_c + R_b + R_s^2 = 1$. The other two equations given above approximate the mean of the test data.

Figures 20, 21, and 22 give a plot of the test results when the cylinders are divided into three groups with different L/D ratio. The curves for the two equations $R_c + R_b + R_s^{2.5} = 1$ and $(R_c + R_b^{1.1})^{1.1} + R_s^{2.5} = 1$ are plotted on the various groups of these figures.

Figure 23 shows how the test data plots when the load ratio R_s is kept constant. The plotted values were obtained by using the curves in figures 16, 17, and 18 and reading off values of R_c and R_b for a constant series of values of R_s equal to 0.2 , 0.4 , 0.6 , and 0.8 , respectively.

Figures 24, 25, and 26 show a similar plot of the test data for the cylinders divided into three groups of different L/D ratio. The results show that the mean of the test results is closely approximated by equation $R_c + R_b + R_s^{2.5} = 1$

or $(R_c + R_b^{1.1})^{1.1} + R_s^{2.5} = 1$. The equation $R_c + R_b + R_s^2 = 1$ represents rather approximately the lower range of the test data. On figure 24 on the upper two series is plotted the curve for the equation $R_c + R_b^{1.5} + R_s^2 = 1$. The result shows that using the exponent of R_b as was found to check mean results in combined bending and torsion is definitely not right for the equation for the three combined loads of compression, bending, and torsion.

Results, Combined Tension and Pure Bending

Near the end of the actual test program it was decided to run a few tests of cylinders with axial tension replacing axial compression.

Figure 27 shows a plot of the test results on two cylinders in combined tension and pure bending. The tension load ratio is given in terms of the compression load ratio R_c and is noted as a negative compression. Thus, when the tension load reached the magnitude of the ultimate compressive strength of the cylinder the load ratio R_c was noted as -1.0. Tension loads greater than that were not applied because of danger of breaking the wire thread in the loading system.

Since there are test results for only two cylinders, the true shape of the interaction is doubtful. Figure 27 indicates that the mean value of the test values is approximated by the equation $R_b + 0.9 R_c = 1$.

Results, Combined Tension and Pure Torsion

Figure 28 shows the test results for the same two cylinders in combined tension and torsion. In the tension region the results of the tests are closely approximated by the equation $R_s + 0.4 R_c = 1$.

Results, Combined Tension, Pure Bending, and Pure Torsion

Figures 29 and 30 show a plot of the test results for test cylinders 13a and 13b loaded in combined tension, bending, and torsion. Curves which simulate this data are drawn

on these figures. In running the tests the tension load was kept constant for a series of tests.

Figures 31 and 32 show a plot of the same test data, but using the load ratio R_s as constant instead of R_c . Thus on figures 29 and 30 constant values of R_s were assumed and corresponding values of R_c and R_b were read from the figures assuming that the curves as drawn on figures 29 and 30 approximated the test data.

On figures 31 and 32 the test points are compared with the curves for the interaction equations $R_c + R_b + R_s^{2.5} = 1$ and $R_c + R_b + R_s^2 = 1$. Although test results are given for only two cylinders the indications are that the interaction equations in the compressive range hold good for the tension range at low values of the tension load, since the maximum tension load used was equal to the strength in pure compression.

Conclusions on Results of Combined Loading Tests

Table A on the following page gives a summary of the various interaction equations which closely approximate the test data for the various combined loadings.

For a circular thin-walled cylinder in combined compression, bending, and torsion, the curve which represents the mean test results fairly well is given by the equation:

$$(R_c + R_b^{1.1})^{1.1} + R_s^{2.5} = 1 \quad (1)$$

For combined compression and pure bending - that is, $R_s = 0$, equation (1) reduces to

$$R_c + R_b^{1.1} = 1 \quad (2)$$

For combined compression and pure torsion - that is, $R_b = 0$, equation (1) reduces to

$$R_c^{1.1} + R_s^{2.5} = 1 \quad (3)$$

For combined pure bending and pure torsion - that is, $R_c = 0$, equation (1) reduces to

TABLE A.- SUMMARY OF INTERACTION EQUATIONS BASED ON TEST DATA

Type of loading	L/D ratio	Interaction equations		
		Lower limit of test values	Mean value of test results	Reference figures
Combined compression and pure bending	0.5, 1.0	$R_c + R_b = 1$	$R_c + R_b^{1.1} = 1$	10, 11
	1.5, 2.0	$R_c + R_b = 1$	$R_c + R_b^{1.1} = 1$	10, 11
Combined compression and pure torsion	0.5, 1.0	$R_c + R_s^2 = 1$	$R_c^{1.1} + R_s^{2.5} = 1$ or $R_c + R_s^{2.5} = 1$	12, 13
	1.5, 2.0	$R_c^{1.1} + R_s^{2.5} = 1$	$R_c^{1.3} + R_s^{2.5} = 1$	12, 13
Combined pure bending and pure torsion	0.5, 1.0	$R_b + R_s^2 = 1$	$R_b^{1.21} + R_s^{2.5} = 1$ or $R_b^{1.5} + R_s^2 = 1$	14, 15
	1.5, 2.0	$R_b^{1.75} + R_s^{1.75} = 1$	$R_b^2 + R_s^2 = 1$	14, 15
Combined compression, pure bending, and pure torsion	0.5, 1.0	$R_c + R_b + R_s^2 = 1$	$R_c + R_b + R_s^{2.5} = 1$ or $(R_c + R_b^{1.1})^{1.1} + R_s^{2.5} = 1$	16 to 26
	1.5, 2.0	$R_c + R_b + R_s^2 = 1$	$R_c + R_b + R_s^{2.5} = 1$ or $(R_c + R_b^{1.1})^{1.1} + R_s^{2.5} = 1$	
Combined tension and pure bending ¹			$^2R_b + 0.9 R_c = 1$	27
Combined tension and pure torsion ¹			$^2R_s + 0.4 R_c = 1$	28
Combined tension, bending, and torsion ¹		$R_c + R_b + R_s^2 = 1$	$^2R_c + R_b + R_s^{2.5} = 1$	31, 32

¹Based on tests of only two cylinders.²A tension load is considered in terms of a negative R_c . Equation only good for small tension loads.

$$R_b^{1.21} + R_s^{2.5} = 1 \quad (4)$$

The results indicated that the curves for equations (1) to (5) approximated the test results in the various conditions of combined loadings. Thus interaction equation (1) can be taken as the general equation applicable to any combination of compression, bending, and torsion. (For closer approximations, see equations in table A.)

In summary table A, two different equations are given in some cases as representing the mean test data. In general, the curve of one of the equations checks the test data better over one portion of the test range, whereas the other equation checks the test results better over the remaining portion. In general, the difference between the curves for the two equations is relatively small.

For quite conservative design for thin-walled circular cylinders where the L/D ratio is 1.0 or less, the test results indicate the following equations for the ultimate strength interaction curves.

Combined compression and pure bending:

$$R_c + R_b = 1$$

Combined compression and pure torsion:

$$R_c + R_s^2 = 1$$

Combined pure bending and pure torsion:

$$R_b + R_s^2 = 1$$

Combined compression, pure bending, and pure torsion

$$R_c + R_b + R_s^2 = 1$$

If the approximate mean of the test results is used for design purposes, the resulting design interaction equations for each of the above conditions of loading, respectively, would be,

$$R_c + R_b^{1.1} = 1$$

$$R_c^{1.1} + R_s^{2.5} = 1$$

$$R_b^{1.2} + R_s^{2.5} = 1$$

$$(R_c + R_b^{1.1})^{1.1} + R_s^{2.5} = 1 \quad \text{or} \quad R_c + R_b + R_s^{2.5} = 1$$

which is slightly more conservative.

For long cylinders (L/D equal to 1.5 to 2.0), the test data plotted higher and the approximate interactions equations are listed in table A. In normal fuselage construction the intermediate transverse frames or rings would usually give a L/D ratio for the cylinder less than 1.0.

The writer thinks that the test values on the celluloid cylinders as a whole tend to lean toward the conservative side because the ultimate buckling strength of the cylinders decreases slightly under repeated failures. Most of this gradual decrease is taken care of by repeating load tests in pure compression, bending, and torsion acting separately at frequent intervals and using the new values if different in calculating the load ratios R_c , R_b , and R_s . (See tables in the appendix for this procedure.)

Furthermore, in the combined tests involving compression, bending, and torsion, the bending and torsion loads were applied simultaneously through one load system and the compression load was run on through a separate system. Since it was convenient to use constant values of R_c in running the tests, the compression load was run on a little faster than the other two load systems, thus the cylinder was carrying the entire test compression load a few seconds before the entire bending and torsion load which caused failure had been added. (This fact it is believed would tend to decrease slightly the true cylinder strength under the combined loads, thus it is thought that the interaction equations based on the mean results of the tests can be assumed as design interaction equations for circular thin-walled cylinders under combined loadings.) The reader should also refer to the general conclusions in part I of this report.

Tests of Cylinders under Combined Transverse Cantilever Bending, Compression, and Pure Torsion

For a number of the test cylinders, the pure bending load system was replaced by cantilever bending which therefore caused flexural shear stresses on the cylinder. The bending moment on the cylinder was produced by applying a side load to the free end of the cylinders. At the same time a compressive and torsional load was applied. Although a considerable number of tests were run, it is thought that the data were not extensive enough to draw definite conclusions regarding expressions for interaction curves.

To illustrate some of the test results, figures 33 and 34 are presented. These figures show the plot of the test results for test cylinders 6b and 15 when subjected to combined compression, cantilever bending, and pure torsion. The term R_p represents the load ratio for cantilever bending. The curves which have been plotted through the test points have a considerably different shape from those in figures 16, 17, and 18, where pure bending was used instead of cantilever bending.

Purdue University,
Lafayette, Ind., May 29, 1944.

APPENDIX

Typical Test Data

To record the complete test data for all the test cylinders would require a considerable number of pages and tables. To illustrate the form of the test data, the results for two test cylinders are presented in this appendix. The meaning of the table column headings is as follows:

- C_m axial compressive load on cylinder which caused failure under pure compression, pounds
- C axial compressive load on cylinder during a combined load test, pounds
- R_c load ratio on compression $\left(\frac{C}{C_m}\right)$

- R_m load which measures pure bending couple that caused failure of cylinder under pure bending, pounds
(Actually it represents twice the couple force.)
- B load which measures applied pure bending moment in combined load tests, pounds
- R_b load ratio in pure bending $\left(\frac{B}{B_m}\right)$

If magnitude of actual bending moment is wanted in inch-pounds, multiply B_m by 10.3 for 7-inch diameter cylinders and by 16.4 for 12-inch diameter cylinders. This takes care of couple arm and friction factor in load system.

- T_m load which measures pure torsional couple which caused failure of cylinder in pure torsion, pounds
(The load is actually twice the couple force.)
- T load which measures applied pure torsion moment in combined load tests, pounds
- R_t load ratio in pure torsion $\left(\frac{T}{T_m}\right)$

NOTE: In plotting the test results the load ratio R_t was given the symbol R_s ; $\therefore R_s = \frac{T}{T_m}$

If actual magnitude of torsional moments is wanted, multiply T_m or T by 10.5 inches for 7-inch diameter cylinders and by 16.7 inches for 12-inch diameter cylinders. This takes care of couple arm and friction factor.

- P_m transverse load applied at free end of cylinder which caused failure of cylinder in cantilever bending, pounds
- P transverse applied load in combined load tests
- R_p load ratio in cantilever bending $\left(\frac{P}{P_m}\right)$

As indicated in the tables, the values of C_m , B_m , and T_m were determined, and then a series of combined tests were run, after which values of C_m , B_m , and T_m were

again obtained, followed by another series of tests, and so on. This process no doubt gave a truer value of the load ratio R_C , R_D , and R_t since the ultimate strength of the cylinder changed slightly after repeated loadings, and since all tests were not run at the same room temperature.

TEST DATA
CYLINDER NO. 1b

D = 6.88" L = 6.84 t = .010

C _m	B _m	T _m	P _m	C	B	T	P	R _c	R _b	R _t	R _p	Tem.
64.3	12.5 12.3	11.15										72°
		11.05										72
												72
												77
				52.0	2.60			.831	.234			80
				42.4	3.82			.676	.345			80
				35.7	4.70			.575	.425			81
				27.7	6.03			.454	.553			81
62.2												85
												80
				25.8	6.38			.421	.586			86
				14.3	8.35			.228	.766			85
62.1	11.05											80
63.3	11.45			48.1	2.77			.776	.251			80
				27.1	6.32			.436	.571			81
												80
												80
		11.45										78
	13.11				13.11	3.98			1.000	.350		74
					8.48	8.48			.650	.747		74
					10.76	6.96			.820	.612		73
	12.85				4.16	10.31			.320	.908		73
		11.11										80
					2.39	10.71			.186	.964		80
					3.19	10.38			.248	.935		80
					4.06	10.05			.316	.905		80
					5.03	9.75			.395	.885		80
					6.01	9.27			.472	.841		80
					7.71	8.81			.558	.800		80
					8.27	8.27			.650	.751		80
					9.37	7.56			.736	.686		81
					10.50	6.80			.824	.617		81
					11.65	5.98			.915	.547		81
					12.31	4.92			.965	.450		81
					12.59	3.82			.988	.344		81
					12.89	2.83			1.000	.259		81
					12.74	1.87			.991	.171		82
					12.73	1.04			.990	.096		82
					1.62	10.73			.128	.982		82
					.93	10.81			.074	.988		82
	12.61											82
		10.93										82
		10.31										86
	11.53											86
					9.89	1.51			.859	.146		86
					9.59	2.17			.832	.210		86
					9.57	2.96			.830	.287		86
					7.70	3.15			.669	.306		86
	10.95											82
		10.33										82

Cylinder 1b cont. next page

TABLE 1

EFFECT OF STRESS AND TIME ON CREEP OF CELLULOID SHEET

Test specimen: $t = 0.0093$ inch
 $b =$ width, 0.253 inch
 gage length, 10 inches

Tension load (grams)	Tension stress (psi)	Unit strain due to creep after various time intervals					Percent creep in 2 minutes, $\frac{\text{unit creep}}{\text{unit strain}}$
		0.25 min.	0.50 min.	1 min.	1.5 min.	2.0 min.	
0	0	-----	-----	0	-----	0	0.0
50	47	-----	-----	0	-----	0	.0
100	94	-----	-----	0	-----	0	.0
200	188	-----	0.000056	.000093	0.000093	.000101	2.55
300	282	-----	.000112	.000112	.000130	.000149	2.55
400	376	-----	.000112	.000224	.000335	.000335	4.40
500	470	-----	.000280	.000465	.000633	.000633	6.80
700	657	-----	.000465	.000652	.000838	.000912	6.80
1000	940	0.000093	.00103	.001250	.001340	.001340	6.90
1500	1410	.000690	.001230	.001750	.002120	.002120	7.44

$\frac{\text{Inches increase after time interval}}{\text{Total inches deflection due to load}} \times 1000$

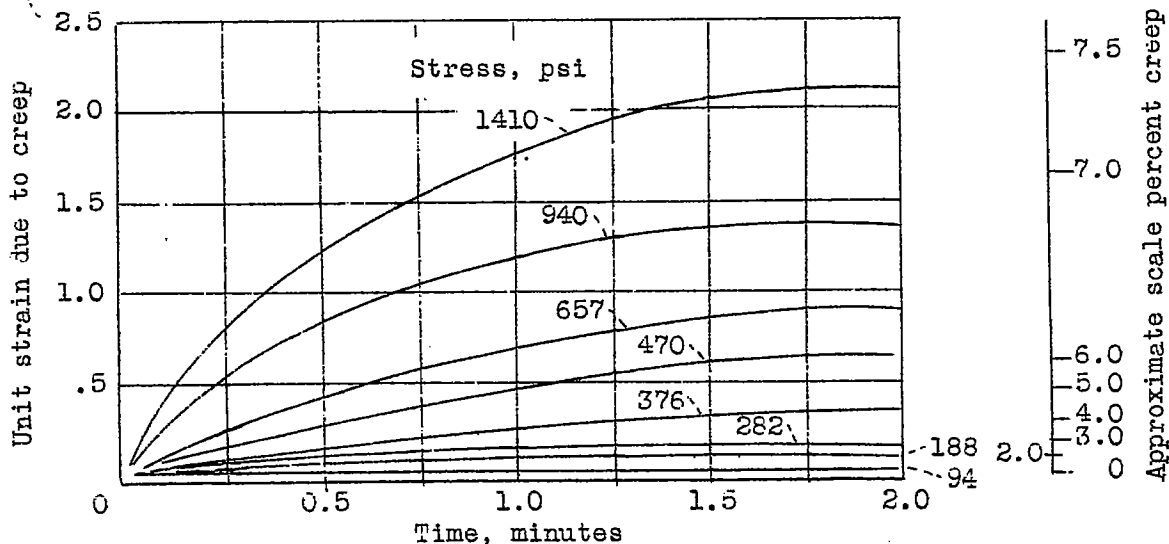
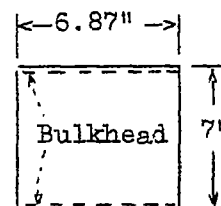


TABLE 2

Cylinder P-1. Length = 7 in., diam. = 6.87, $t = 0.0075$

Bending and torsional strength under repeated loading
with variation in time of loading.



Pure bending tests			Pure torsion tests		
Test No.	Scale load at failure (lb)(oz)	Time of loading (min)	Test No.	Scale load at failure (lb)(oz)	Time of loading (min)
1	3 7.3	0.13	1	3 12.5	0.10
2	3 6.8	.20	2	3 11.8	.17
3	3 5.9	.34	3	3 11.3	.31
4	3 5.8	.65	4	3 11.1	.48
5	3 5.5	.93	5	3 10.0	.78
6	3 5.7	.40	6	3 10.9	.72
7	3 6.1	.26	7	3 10.9	.36
8	3 6.9	.12	8	3 11.3	.23
9	3 7.4	.10	9	3 12.1	.14
Average 3 6.38			Average 3 11.31		

Maximum percent variation from average of 9 tests = 1.88 percent. Percent difference between first and ninth test which had practically the same time of loading = 0.18 percent..

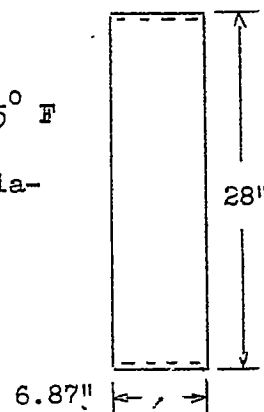
NOTE: When the cylinder buckled, the scale reading dropped, thus the highest reading of the pointer on the scale was read and recorded.

Maximum percent variation from average of 9 tests = 2.2 percent. Percent difference between first and ninth test, which had approximately same time of loading, = 0.66 percent.

TABLE 3

Cylinder P-2. $L = 28$ in., $D = 6.87$ in., $t = 0.0075$, temp. = 75° F

Bending and torsional strength under repeated loading with variation in time of loading.



Pure bending tests			Pure torsion tests		
Test No.	Scale load at failure (lb)(oz)	Time of loading (min)	Test No.	Scale load at failure (lb)(oz)	Time of loading (min)
1	3 8.0	0.81	1	1 12.5	0.20
2	3 8	.20	2	1 13.0	.20
3	3 8	.30	3	1 13.25	.10
4	3 7.8	.40	4	1 12.75	.14
5	3 7.5	.52	5	1 12.60	.15
6	3 8.2	.14	6	1 12.10	.42
7	3 8.2	.11	7	1 12.0	.78
8	3 7.6	.54	8	1 13.00	.09
9	3 8.7	.12	9	1 13.00	.21
10	3 8.7	.36	10	1 12.40	.43
11	3 7.4	.61	11	1 12.60	.61
Average 3 8.0			Average 1 12.68		

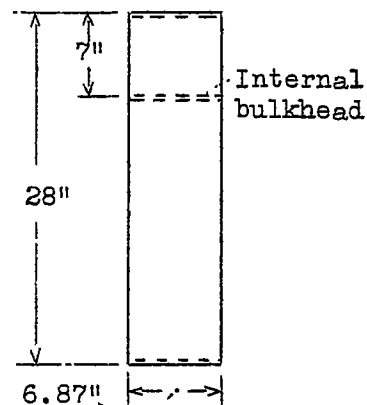
Maximum percent variation from average of 11 tests = 1.25 percent.

Maximum percent variation from average of 11 tests = 1.98 percent.

TABLE 4

Cylinder P-2 (modified). One internal bulkhead added as indicated in sketch.

Bending and torsional strength under repeated loading with variation in time of loading.



Pure bending tests			Pure torsion tests		
Test No.	Scale reading at failure (lb)(oz)	Time of loading (min)	Test No.	Scale reading at failure (lb)(oz)	Time of loading (min)
1	3 8.0	0.27	1	2 1.9	0.17
2	3 7.8	.30	2	2 2.0	.21
3	3 7.9	.24	3	2 2.0	.33
4	3 7.8	.35	4	2 2.0	.22
5	3 7.9	.27	5	2 1.8	.20
			6	2 1.1	.47
			7	2 1.7	.18
Average 3 7.88			Average 2 1.79		

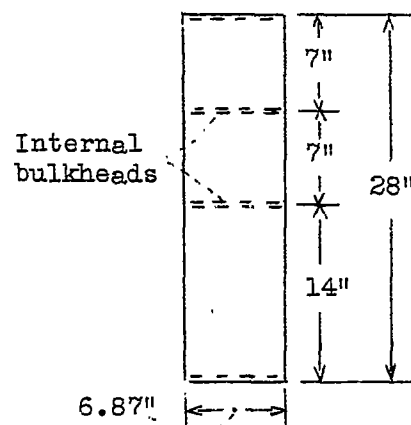
Maximum percent variation from average of 5 tests = 0.14 percent.

Maximum percent variation from average of 5 tests = 2.07 percent.

TABLE 5

Cylinder P-2 (modified). Two internal bulkheads added as indicated in sketch.

Bending and torsional strength under repeated loading with variation in time of loading.



Pure bending tests			Pure torsion tests		
Test No.	Scale reading at failure (lb)(oz)	Time of loading (min)	Test No.	Scale reading at failure (lb)(oz)	Time of loading (min)
1	3 4.0	0.30	1	2 7.4	0.26
2	3 5.7	.25	2	2 7.6	.19
3	3 5.0	.25	3	2 7.5	.25
4	3 4.9	.26	4	2 7.5	.22
5	3 4.5	.32	5	2 7.0	.36
6	3 5.2	.16	6	2 7.6	.16
Average 3 4.9			Average 2 7.39		

Maximum percent variation from average of 6 tests = 1.7 percent.

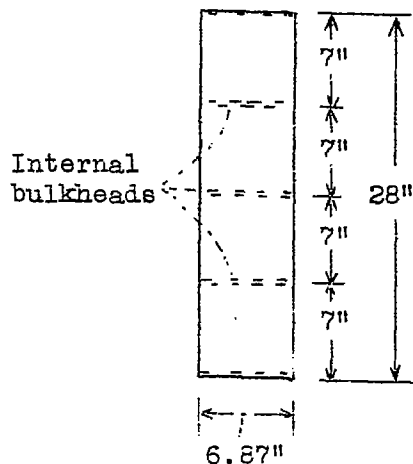
Maximum percent variation from average of 6 tests = 0.99 percent.

TABLE 6

Cylinder P-2 (modified). Three internal bulkheads added as indicated in sketch.

Pure torsion tests		
Test No.	Scale reading at failure (lb)(oz)	Time of loading (min)
1	3 2.2	0.15
2	3 2.2	.25
3	3 2.7	.12
4	3 2.1	.19
5	3 2.2	.20
6	3 2.2	.14
Average	3 2.27	

Maximum percent variation from average of 6 tests = 0.85 percent.



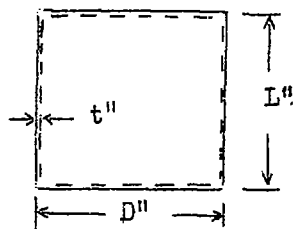
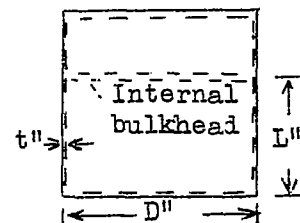


TABLE 7

SUMMARY OF TEST CYLINDER DATA



1	2	3	4	5	6	7	8
Cylinder No.	Test cyl. No.	Diam. D = 2r	t =	r/t	L	L/D	Remarks
1	1a	6.87	0.010	344	3.40	0.495	Cylinder 1b cut down.
	1b	6.87	0.010	344	6.75	0.983	
2	2a	6.88	0.0075	458	6.87	1.00	
	2b	6.88	0.0075	458	3.40	0.495	Cylinder 2a cut down.
3	3a	7.00	0.015	234	7.00	1.00	
	3b	7.00	0.015	234	3.50	0.50	Cylinder 3a cut down.
4	4	7.00	0.015	234	3.50	0.50	
5	5a	6.90	0.010	345	13.80	1.0	One intermediate bulkhead at midpoint.
	¹ 5b	6.90	0.010	345	13.80	1.0	Same as 5a but second series of tests.
	5c	6.90	0.010	345	13.80	.62	Two intermediate bulkheads spaced 8.6 in. apart.
6	6a	6.88	0.010	344	6.81	1.00	
	6b	6.88	0.010	344	3.41	0.50	Cylinder 6a cut down.
7	7a	7.00	0.015	234	10.15	1.45	
	7b	7.00	0.015	234	10.15	0.73	One intermediate bulkhead at midpoint.
8	8a	6.90	0.010	345	13.80	0.67	Two intermediate bulkheads spaced 4.6 in. apart.
	¹ 8b	6.90	0.010	345	13.80	0.67	Same as cylinder 8a.
	8c	6.90	0.010	345	13.80	1.00	Two intermediate bulkheads spaced 6.86 in. apart.

¹Pure bending replaced by cantilever bending due to transverse load at free end.

TABLE 7 (continued)

1	2	3	4	5	6	7	8
Cylinder No.	Test cyl. No.	Diam. D = 2r	t =	r/t	L	L/D	Remarks
9	9a	6.90	0.010	345	10.35	1.50	
	9b	6.90	0.010	345	13.80	0.67	Two intermediate bulkheads spaced 4.56 in. apart.
	9c	6.90	0.010	345	10.35	0.75	Two intermediate bulkheads spaced 5.16 in. apart.
10	10	6.90	0.0075	460	13.8	2.00	
11	11	6.88	0.0075	460	14.0	1.00	One intermediate bulkhead at midpoint.
12	12a	12.00	0.010	600	12.00	1.00	
	12b	12.00	0.010	600	6.00	0.50	
13	13a	12.00	0.0075	800	12.00	1.00	
	13b	12.00	0.0075	800	6.00	0.50	
14	14	12.00	0.0075	800	12.00	1.00	
15	15	12.00	0.010	600	6.00	0.50	
16	16	12.00	0.010	600	11.9	0.99	

Explanation of columns:

Column (1) 16 different official test cylinders were fabricated. These are numbered 1 to 16.

Column (2) For test purposes the 16 cylinders were modified to obtain 29 separate test units. This was done by cutting the original cylinder down to a shorter length or by inserting intermediate bulkheads to change L/D ratio.

Column (3) Diameter of celluloid cylinder, inches.

Column (4) Wall thickness of celluloid cylinders, inches.

Column (5) Radius of cylinder/wall thickness.

Column (6) Cylinder length between center line of end bulkheads.

Column (7) Length/diameter ratio.

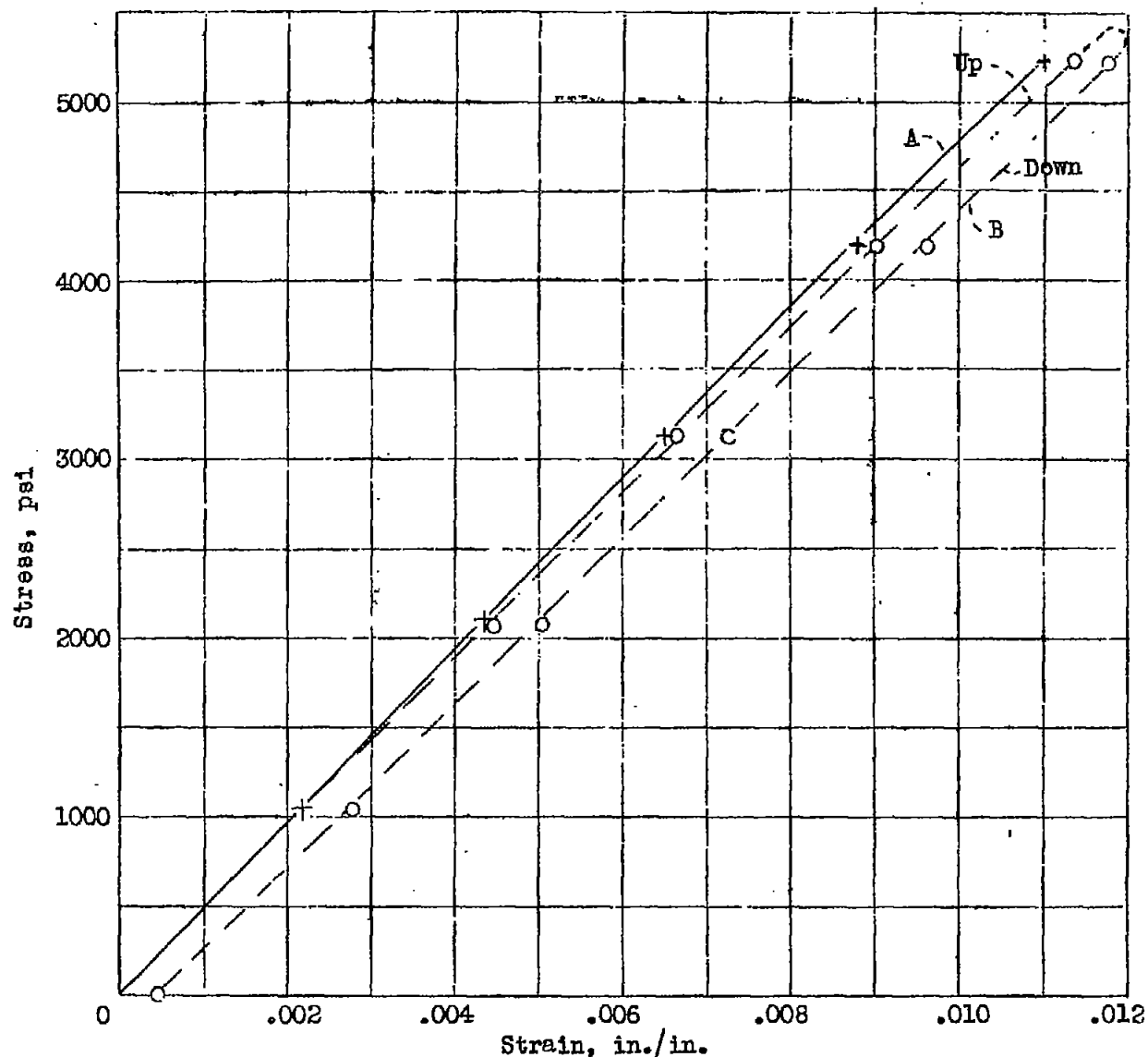
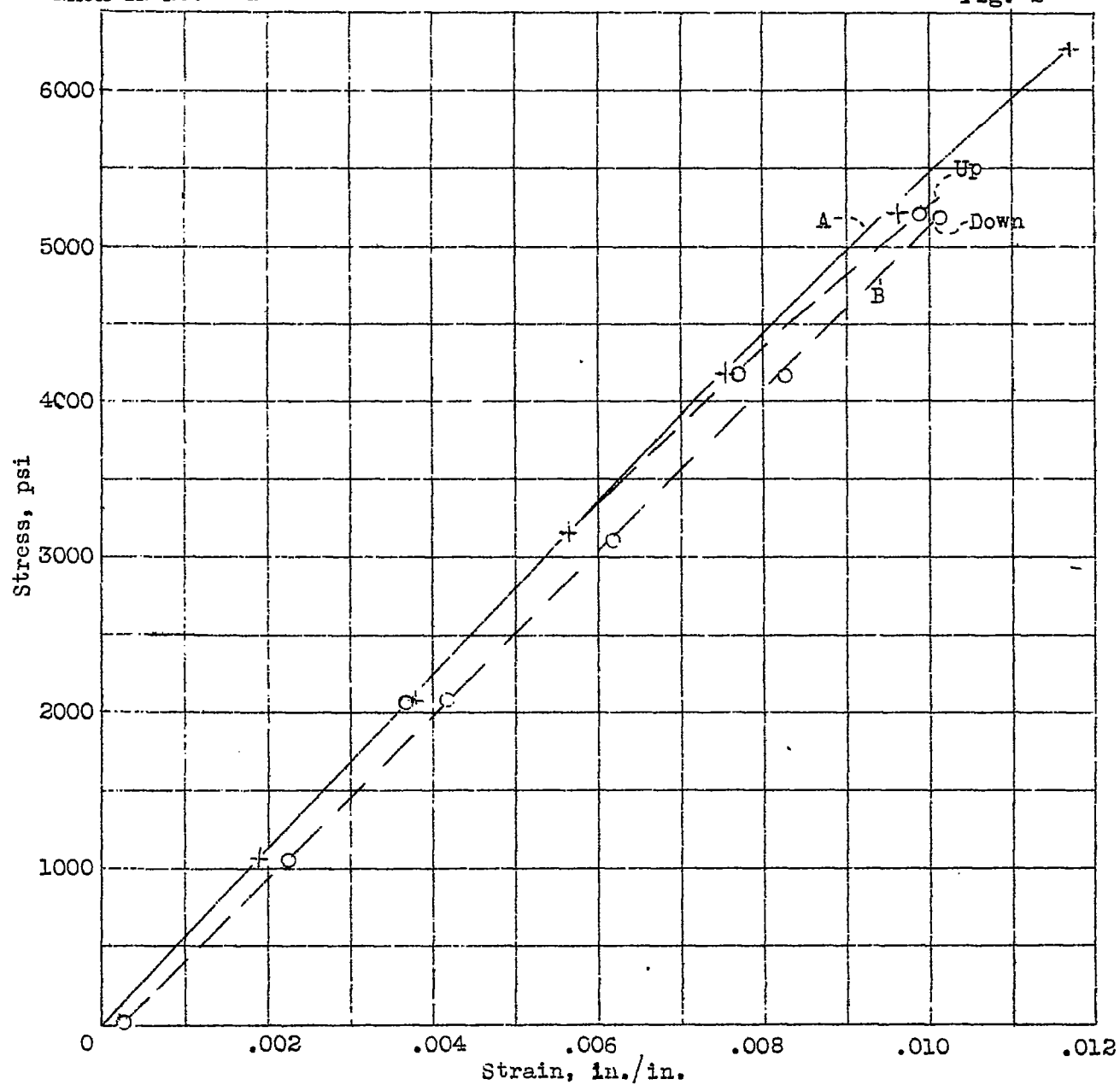


Figure 1.- Tension stress-strain curve for celluloid sheet.



$$E = 555,000 \text{ psi}$$

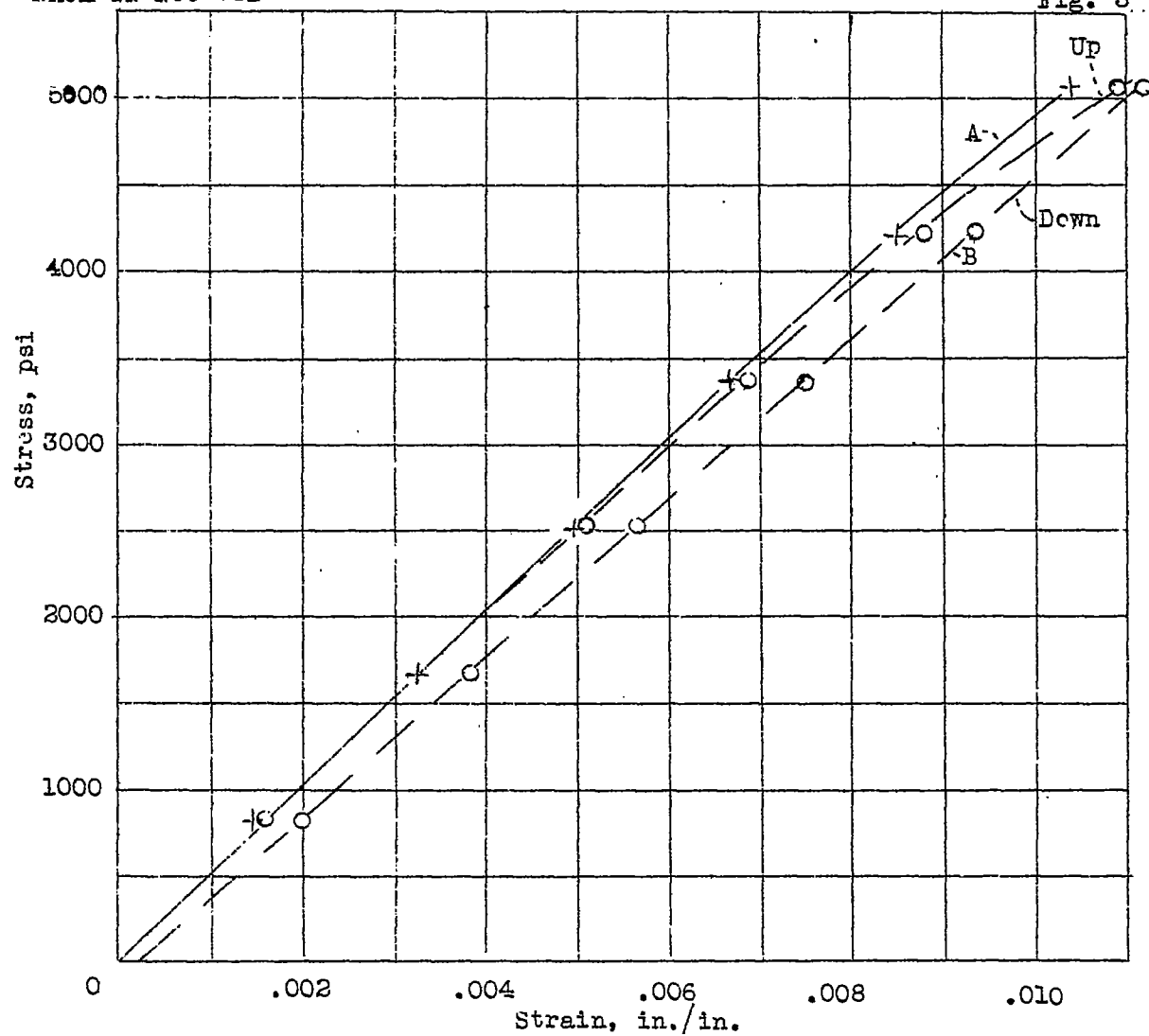
$$t = 0.00738''$$

$$w = 0.265''$$

Specimen cut parallel to width of 20" x 50" sheet

$$\text{Temperature} = 70^{\circ}\text{F}$$

Figure 2.- Tension stress-strain curve for celluloid sheet.

 $E = 506,000 \text{ psi}$ $t = 0.0093''$ $w = 0.253''$

Specimen cut parallel to
long dimension of sheet

 $\text{Temperature} = 70^{\circ}\text{F}$

Figure 3.- Tension stress-strain curve for celluloid sheet.

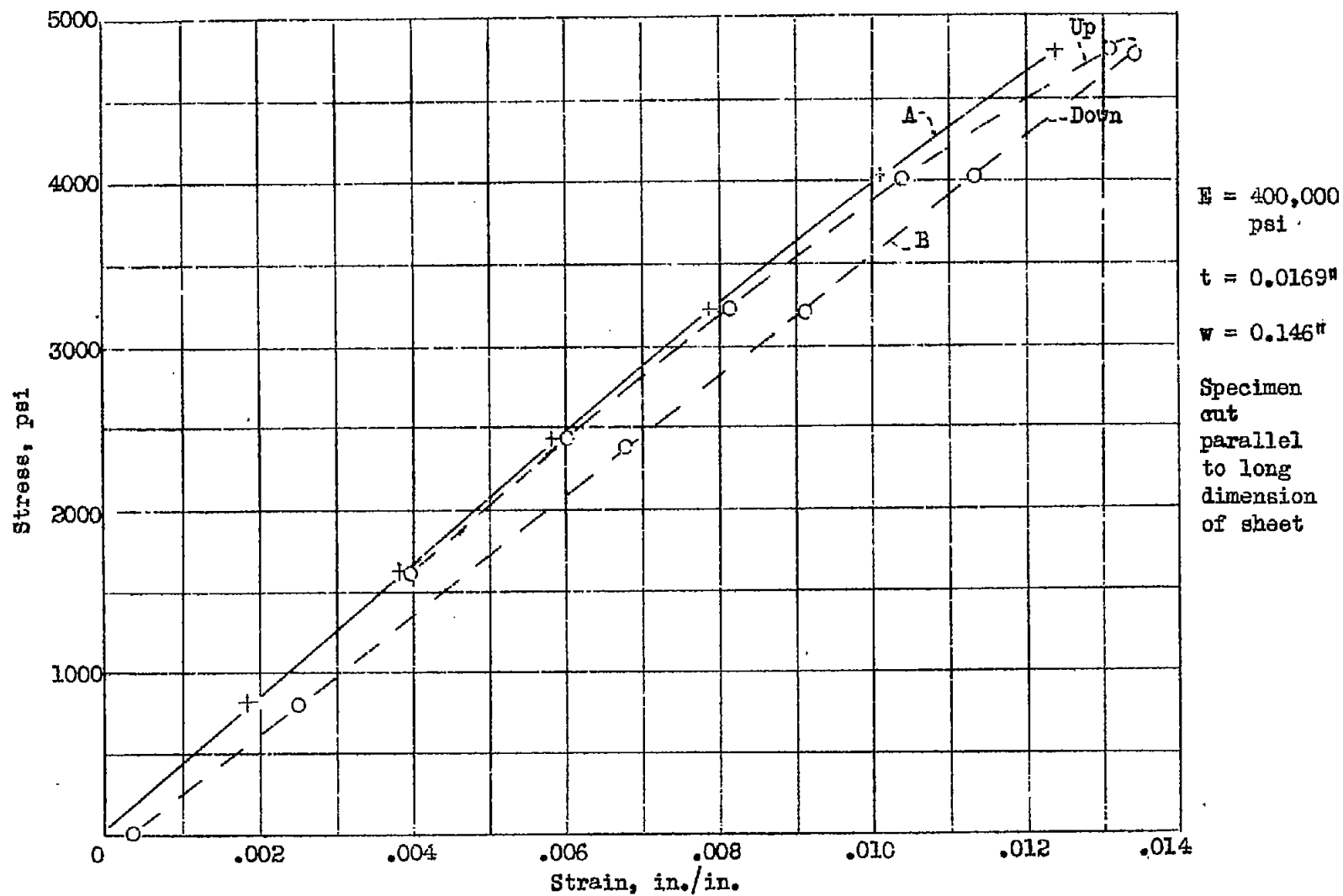


Figure 4.-- Tension stress-strain curve for celluloid sheet.

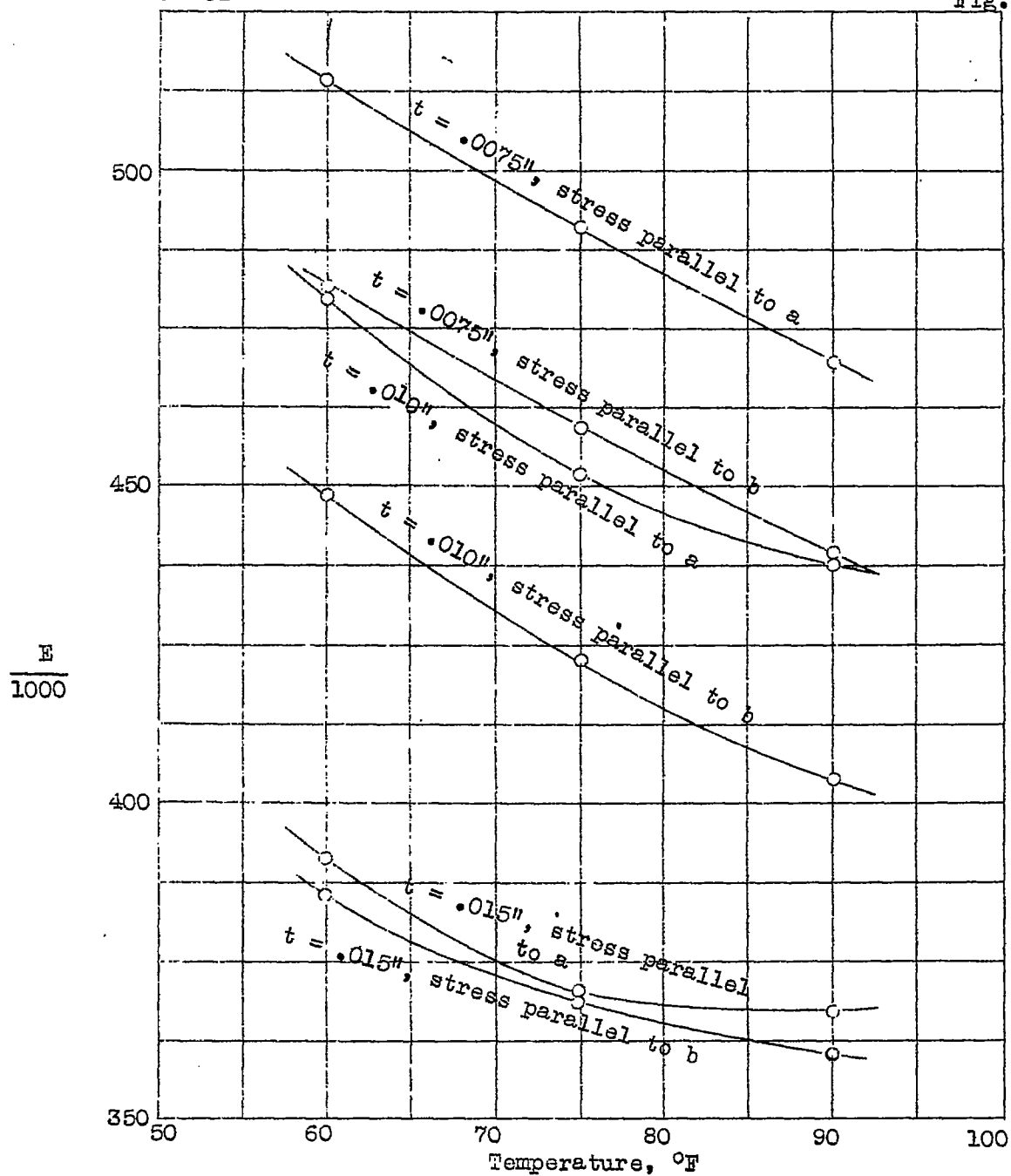


Figure 5.— Variation of stiffness of celluloid sheet with change in room temperature.

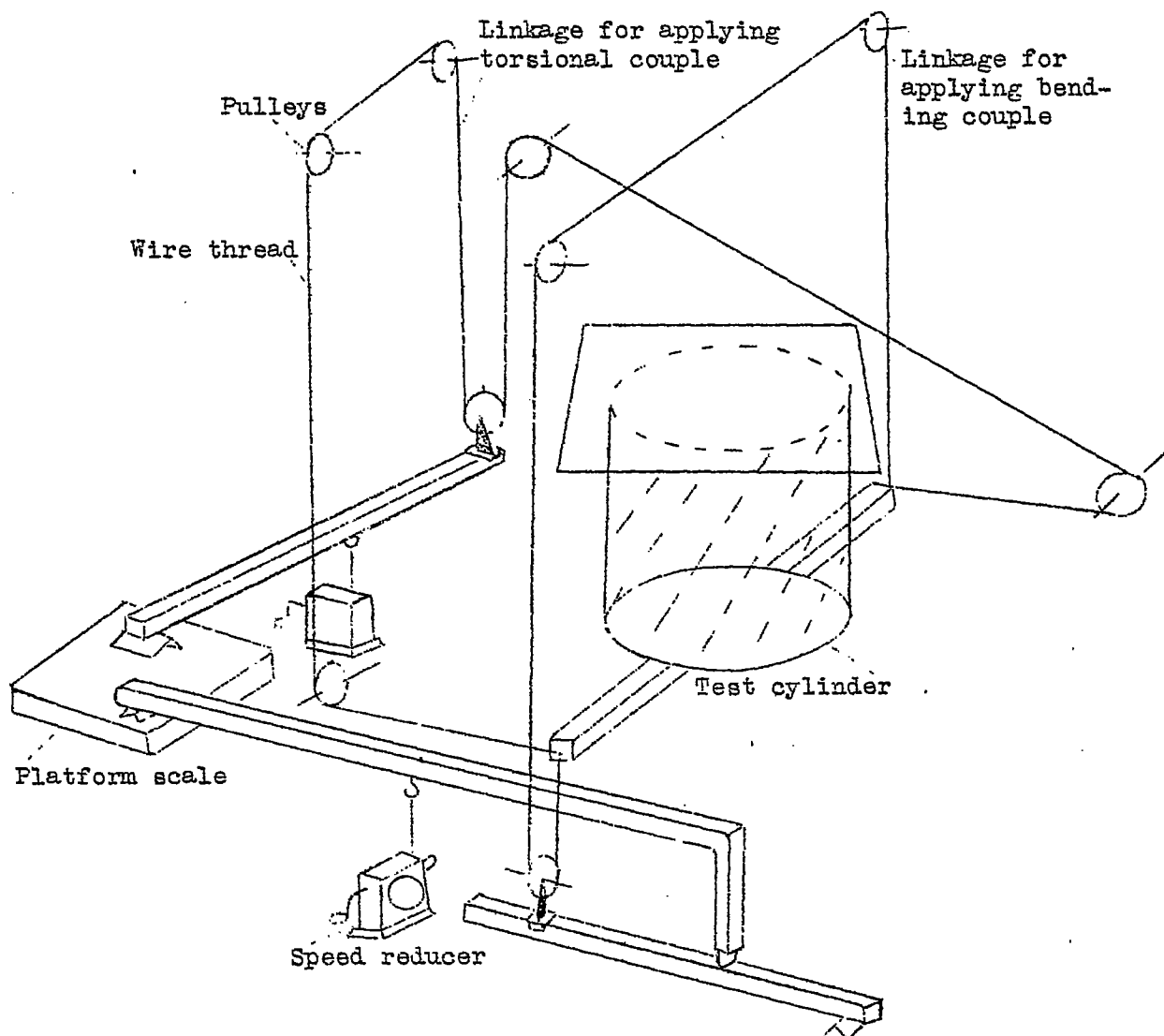


Figure 6.- Schematic diagram of apparatus for applying pure bending and pure torsion to preliminary test cylinders P-1 and P-2.

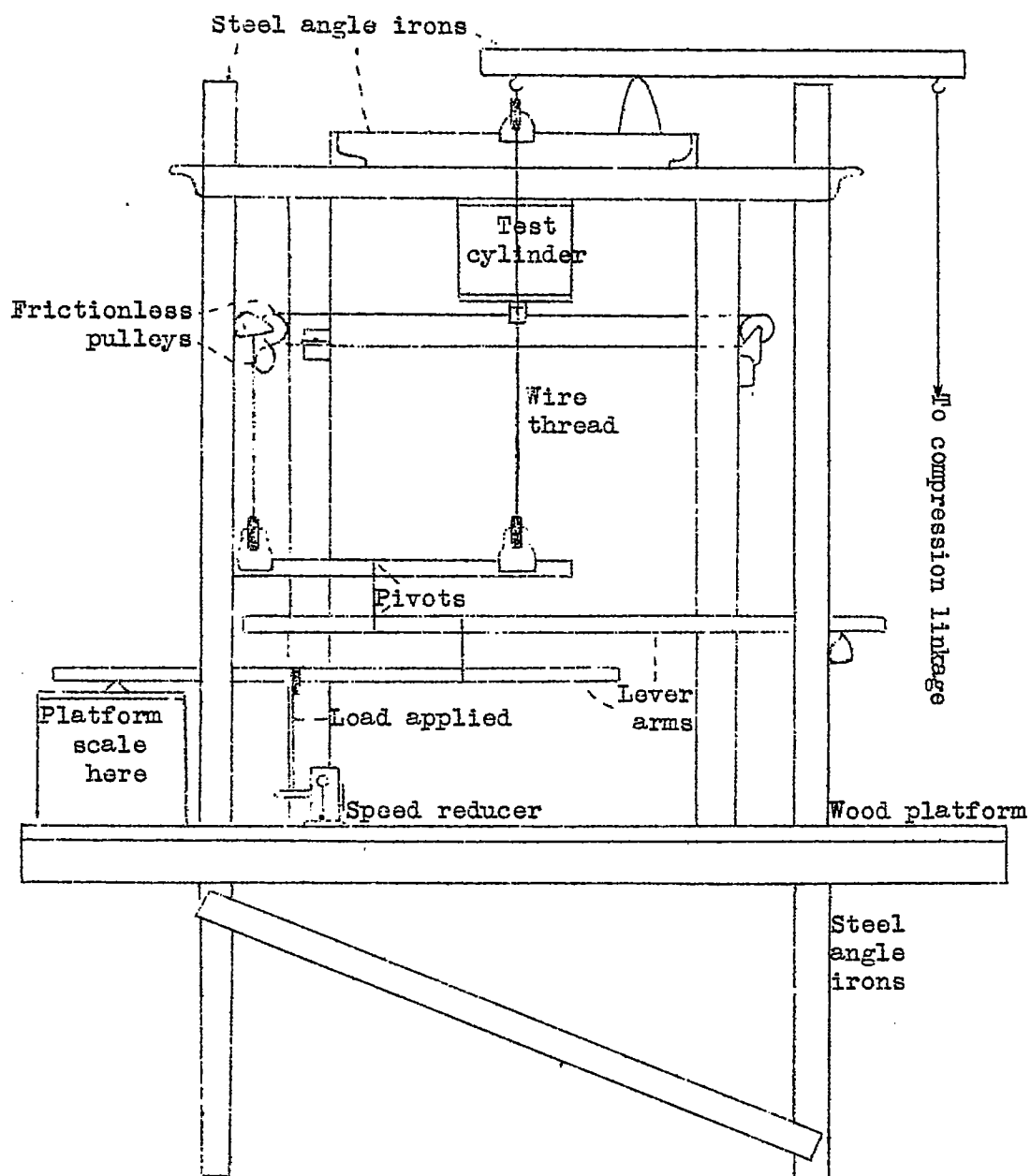


Figure 7.- Sketch of test jig.

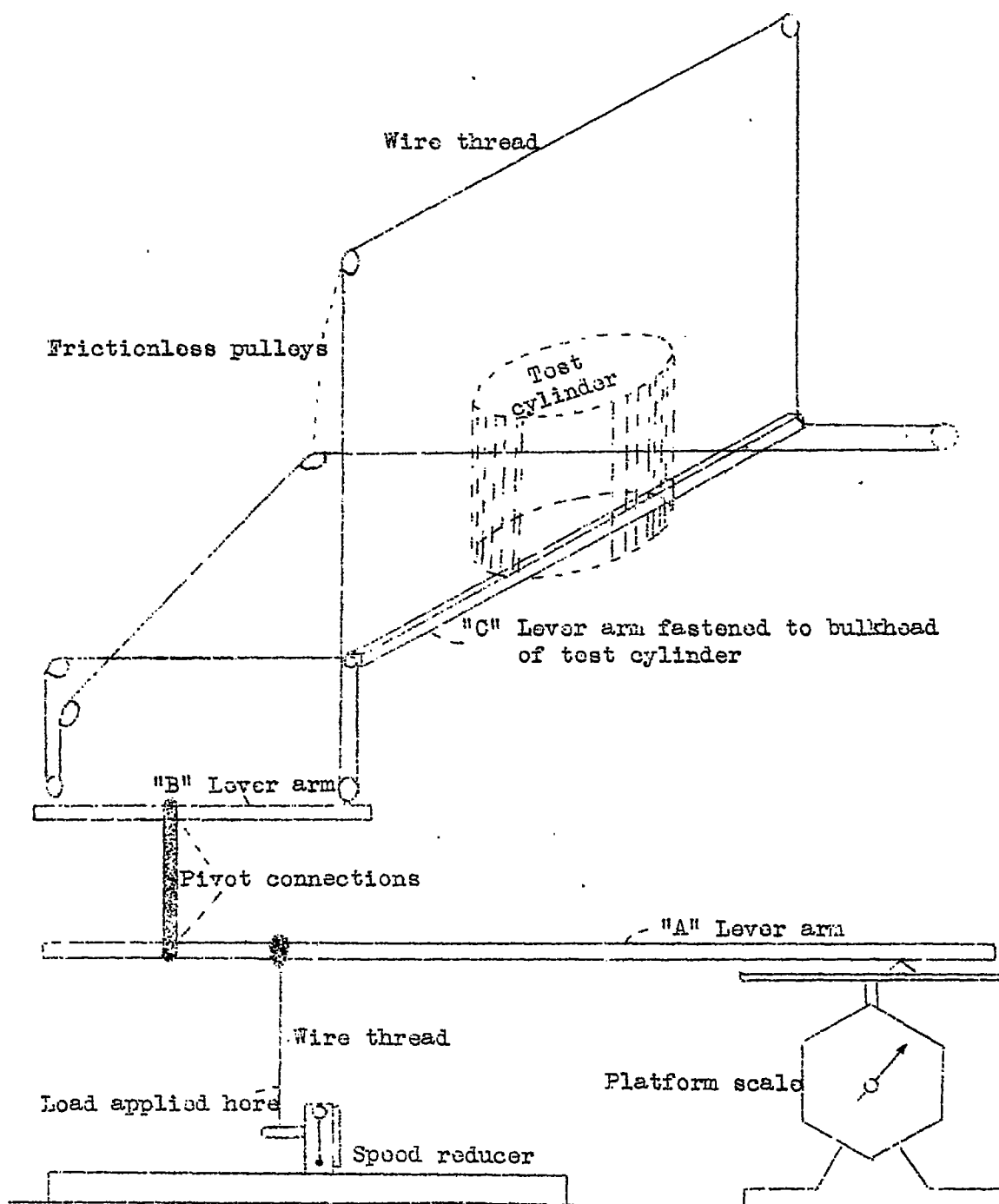


Figure 8.- Schematic diagram of apparatus for applying pure bending and pure torsional loads to cylinders.

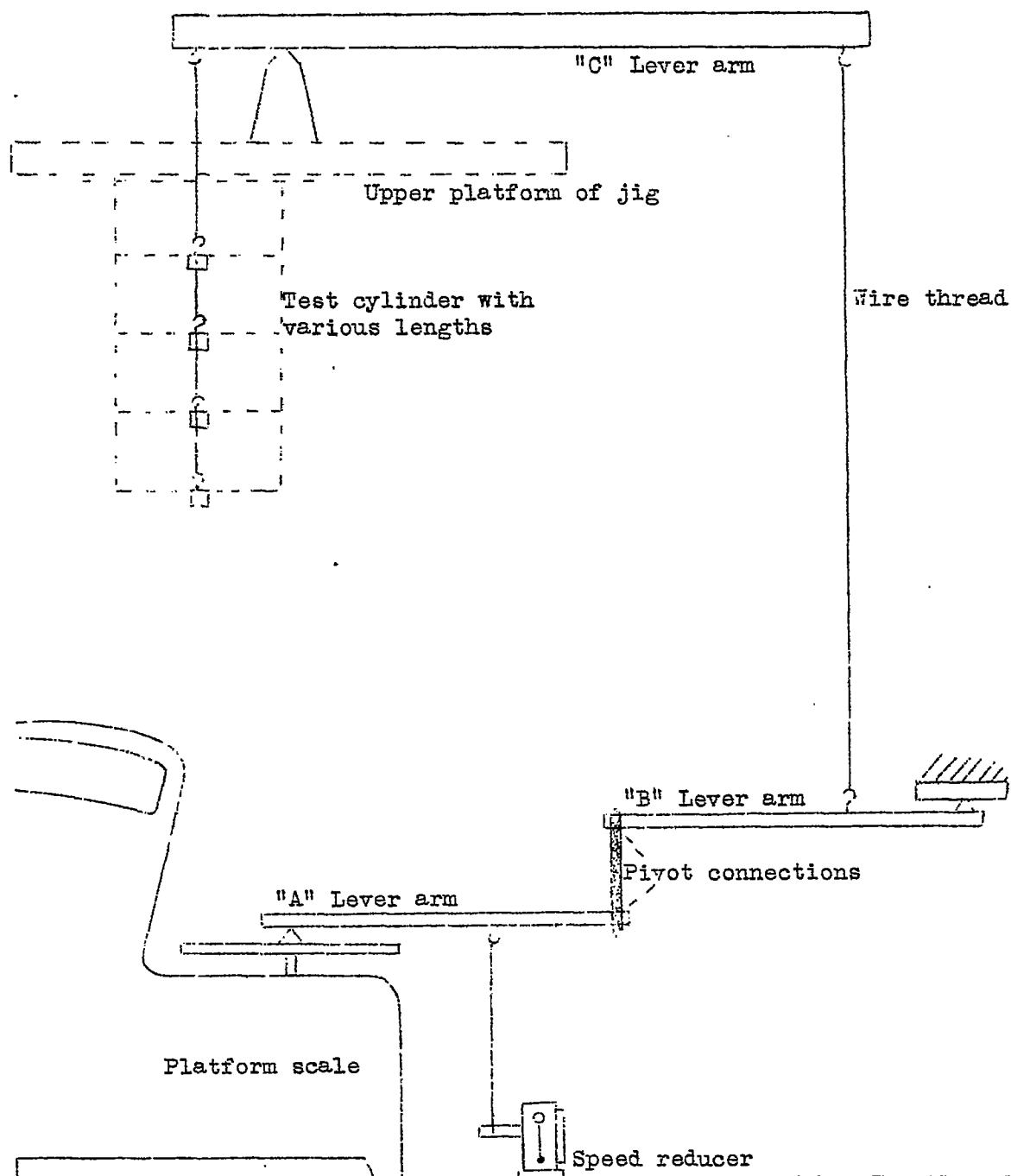
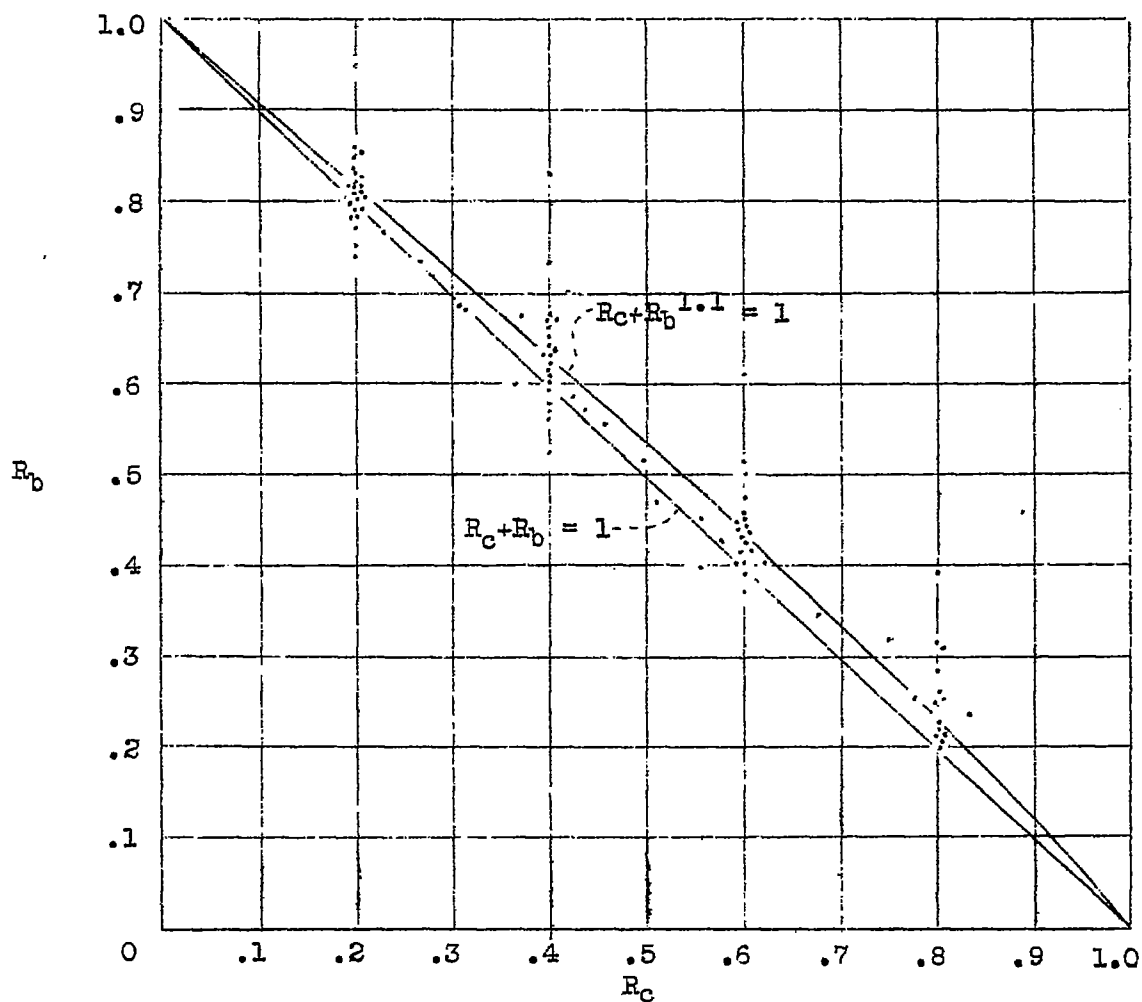
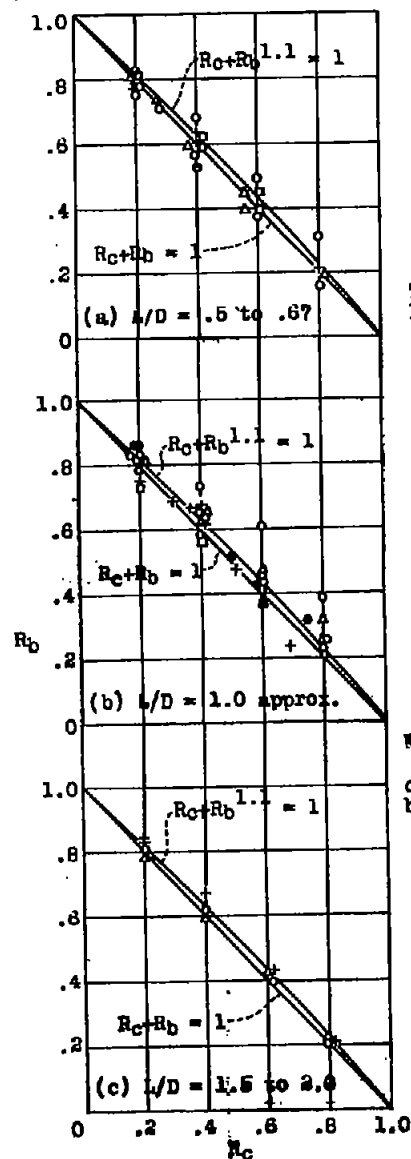


Figure 9.- Schematic diagram of apparatus for applying pure compression loads to cylinder.



(All test values are plotted without distinction for r/t or L/D values of cylinders. See Figure 11 for additional curves).

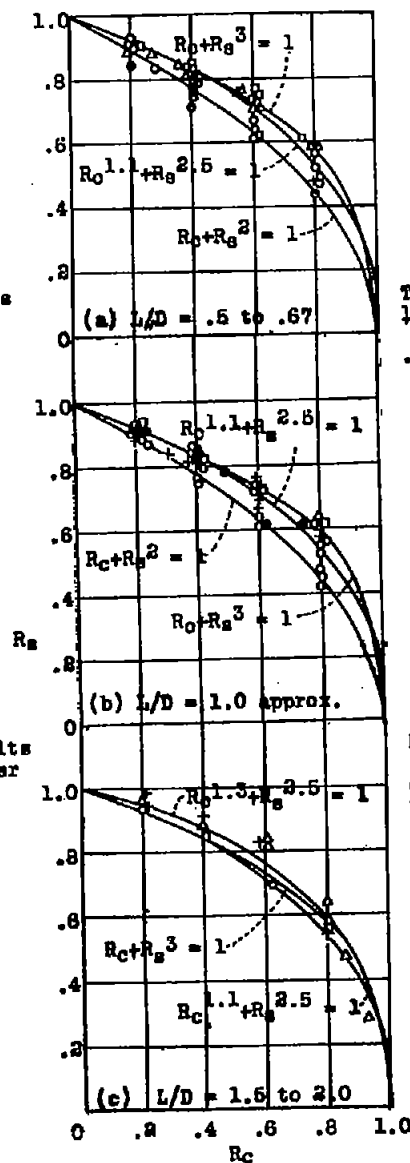
Figure 10.— Plot of test results for cylinders in combined compression and pure bending.



The test data on the cylinders listed below are plotted.

$L/D = .5$ to $.67$	$L/D = 1.0$	$L/D = 1.5$ to 2.0
1a	1b	7a
2b	2a	9a
3b	3a	10
4	5a	
7b	11	
8a	12a	
9b	13a	
12b	9c	
13b		

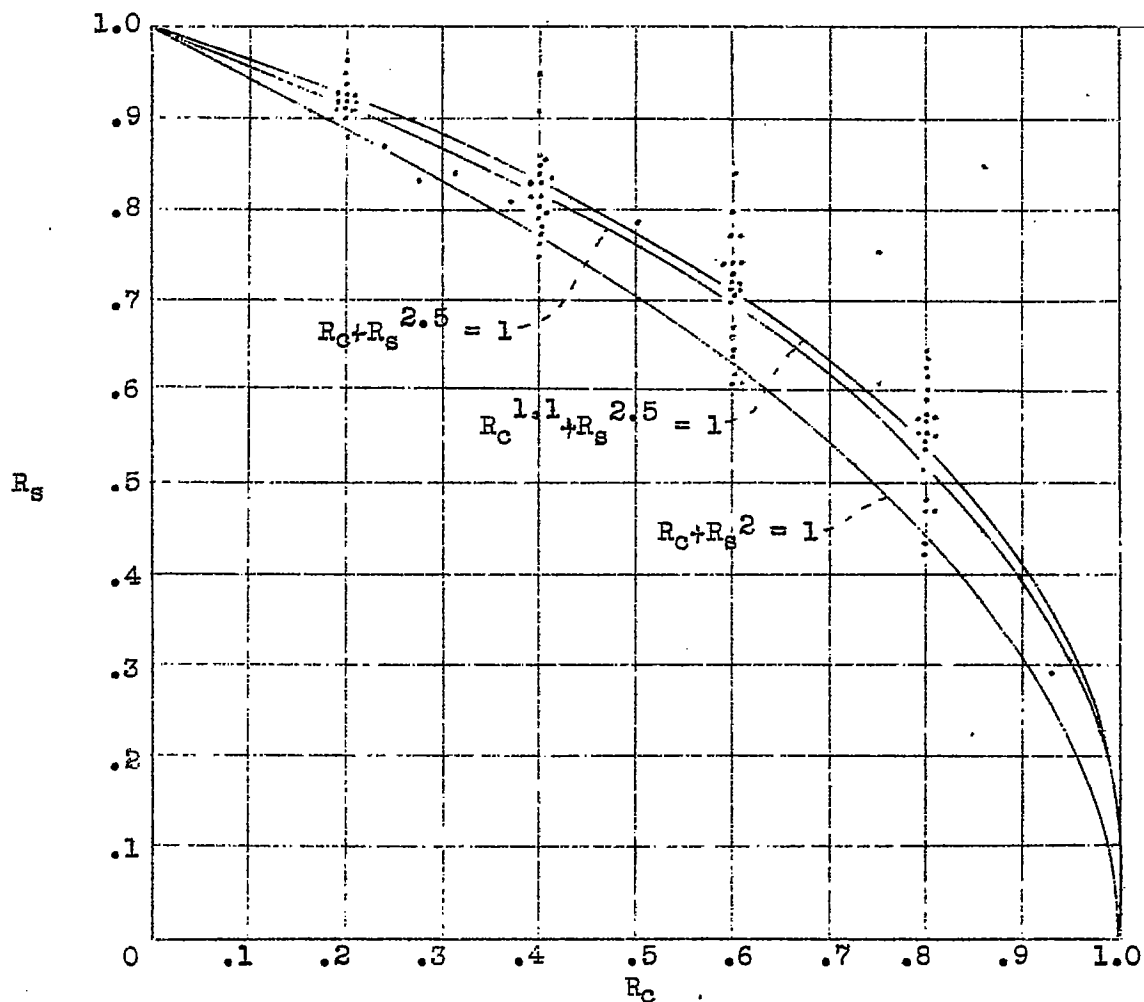
Figure 11.- Plot of test results for cylinders under combined compression and pure bending loads



The test data on the cylinders listed below are plotted.

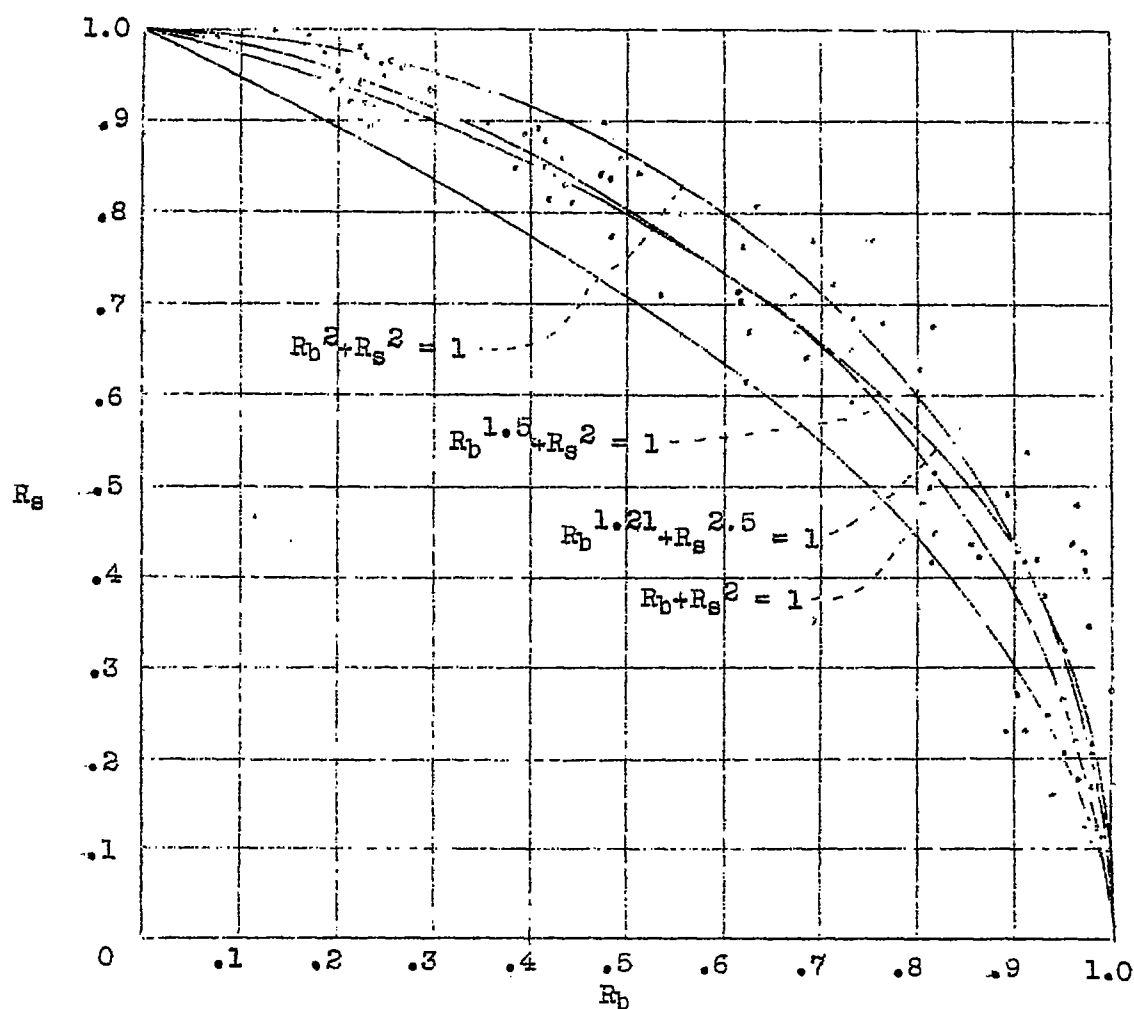
$L/D = .5$ to $.67$	$L/D = 1.0$	$L/D = 1.5$ to 2.0
1a	1b	7a
2b	2a	9a
3b	3a	10
4	5a	
6b	5b	
8a	8c	
8b	9c	
9b	11	
12b	12a	
13b	13a	
15	14	
	16	

Figure 13.- Plot of test results for cylinders under combined compression and pure torsion loads.



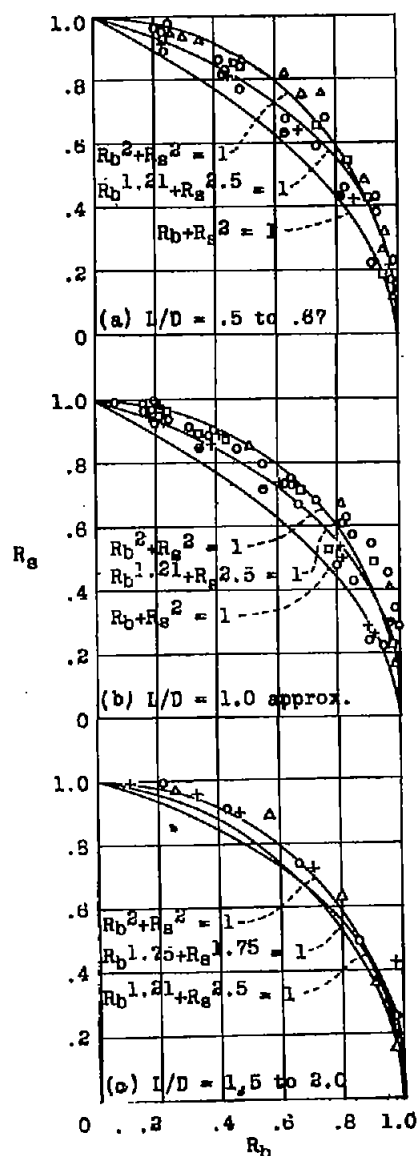
(All values are plotted without consideration of r/t or L/D values of test cylinders. Refer to Figure 13 for these considerations).

Figure 12.- Test results for cylinders loaded in combined compression and pure torsion.



(All values are plotted without consideration of r/t or L/D of test cylinders. Refer to Figure 15 for these considerations).

Figure 14.- Test results for cylinders loaded in combined pure bending and pure torsion.

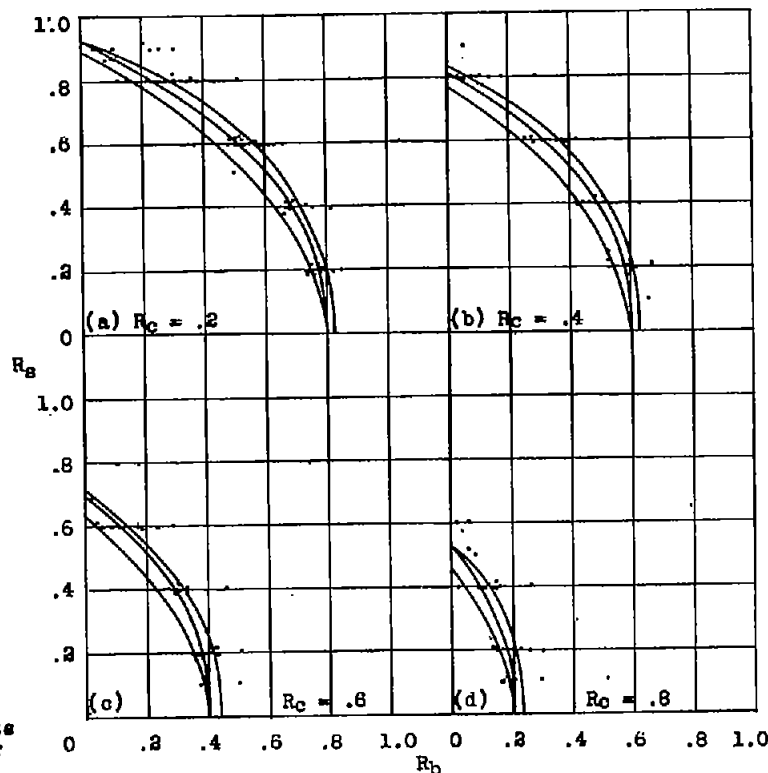


$r/t = 230 = \Delta$
 $r/t = 345 = \circ$
 $r/t = 480 = +$
 $r/t = 600 = \square$
 $r/t = 800 = \Theta$

The test data on the cylinders listed below are plotted.

$L/D = .5 \text{ to } .87$	$L/D = 1.0$	$L/D = 1.5 \text{ to } 2.0$
1a	1b	7a
2b	2a	9a
3b	3a	10
4	5a	
7b	8c	
8a	11	
9b	12a	
12b	9c	
13b		

Figure 15.- Plot of test results for cylinders under combined pure bending and pure torsion loads.



Explanation:

Values of plotted points are obtained from tables in the appendix. Values are plotted without distinction for r/t or L/D of cylinders. See Figures 20, 21, 22 for additional curves.

The diagonal lines as plotted above represent the following interaction equations:

upper line $(R_c + R_b^{1.1})^{1.1} + R_s^{2.5} = 1$

middle line $R_c + R_b + R_s^{2.5} = 1$

lower line $R_c + R_b + R_s = 1$

Figure 19.- Plot of test data for cylinders loaded in combined compression, pure bending, and pure torsion.

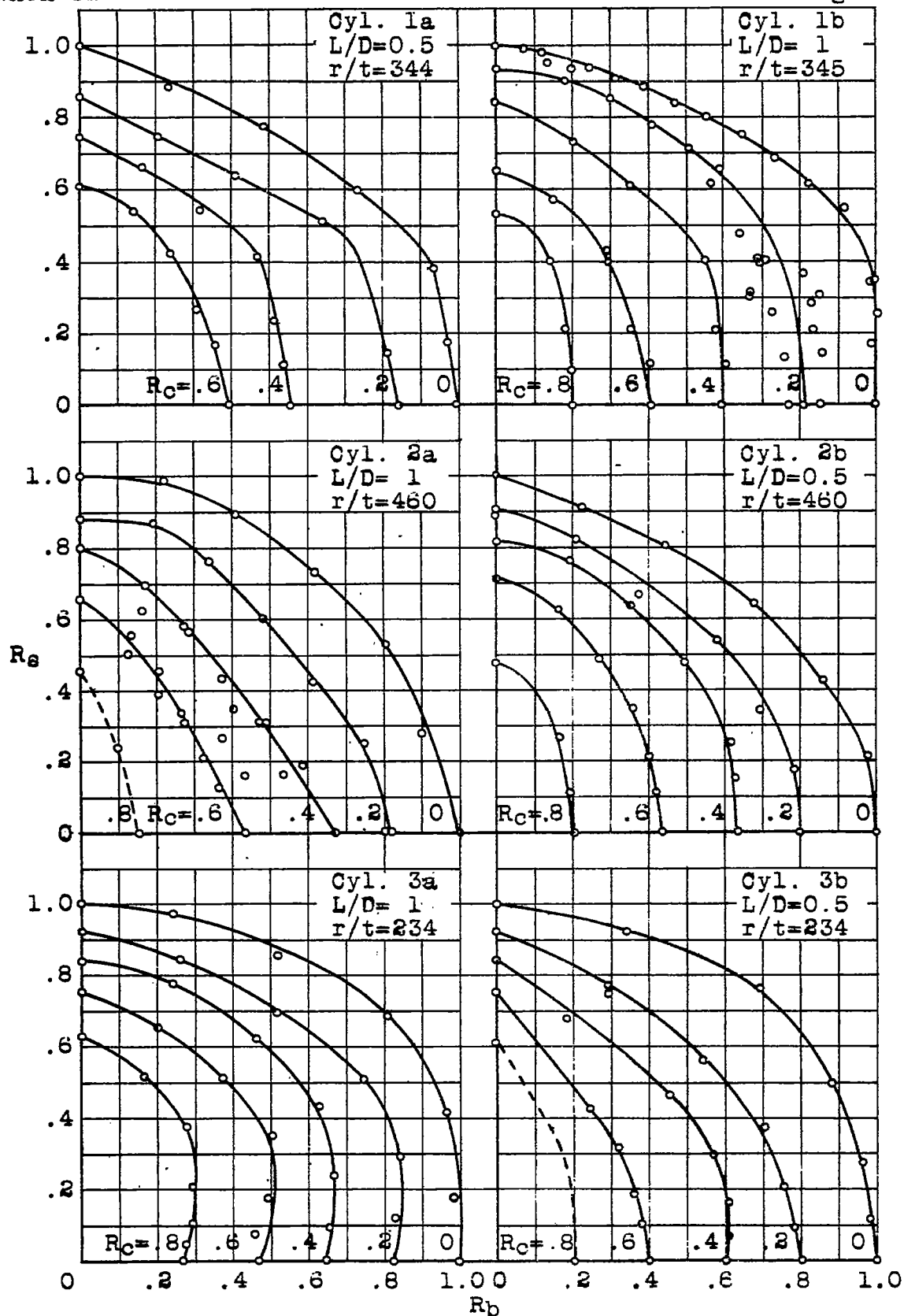


Figure 16.- Plot of test results for various test cylinders loaded in combined compression, pure bending and pure torsion.

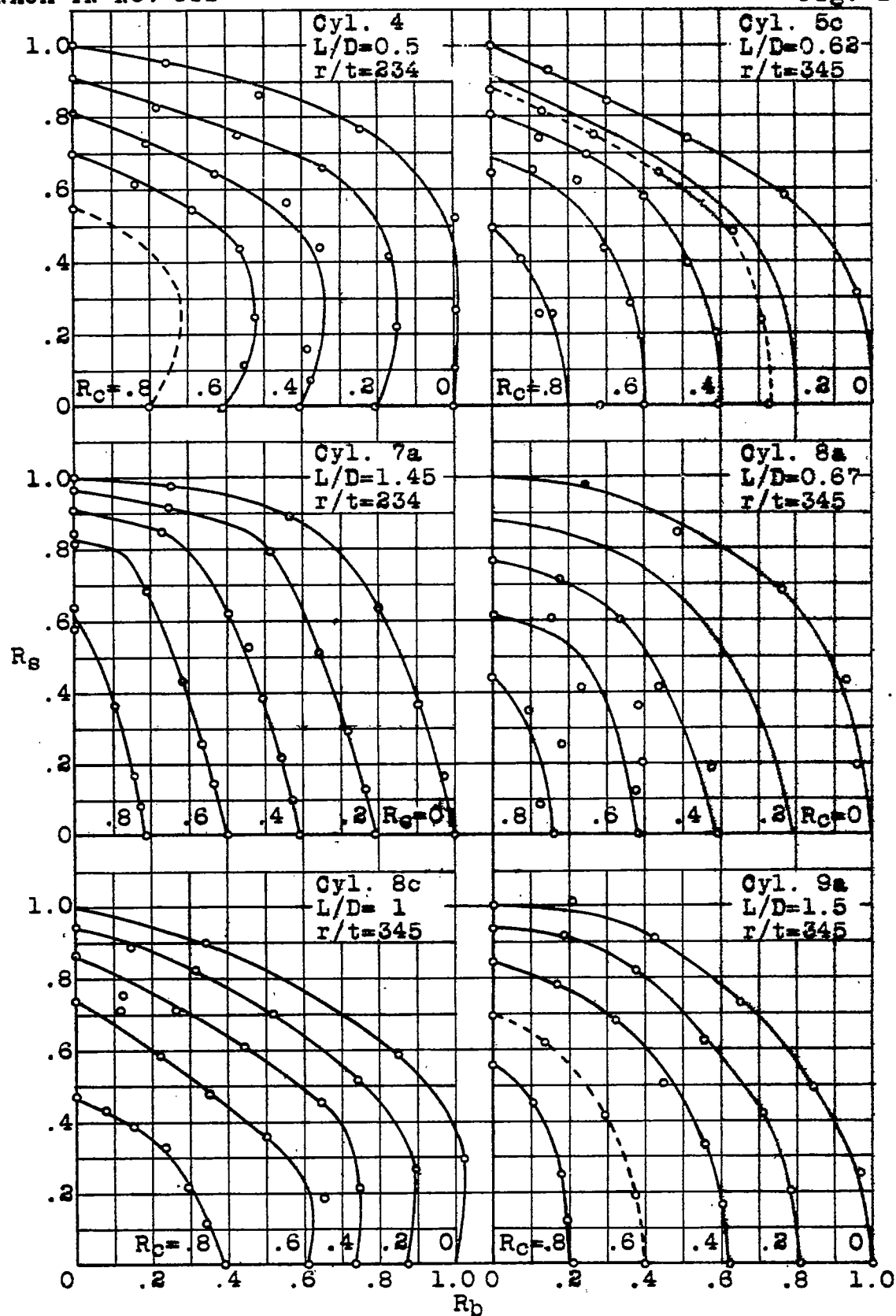


Figure 17.- Plot of test results for various test cylinders loaded in combined compression, pure bending and pure torsion.

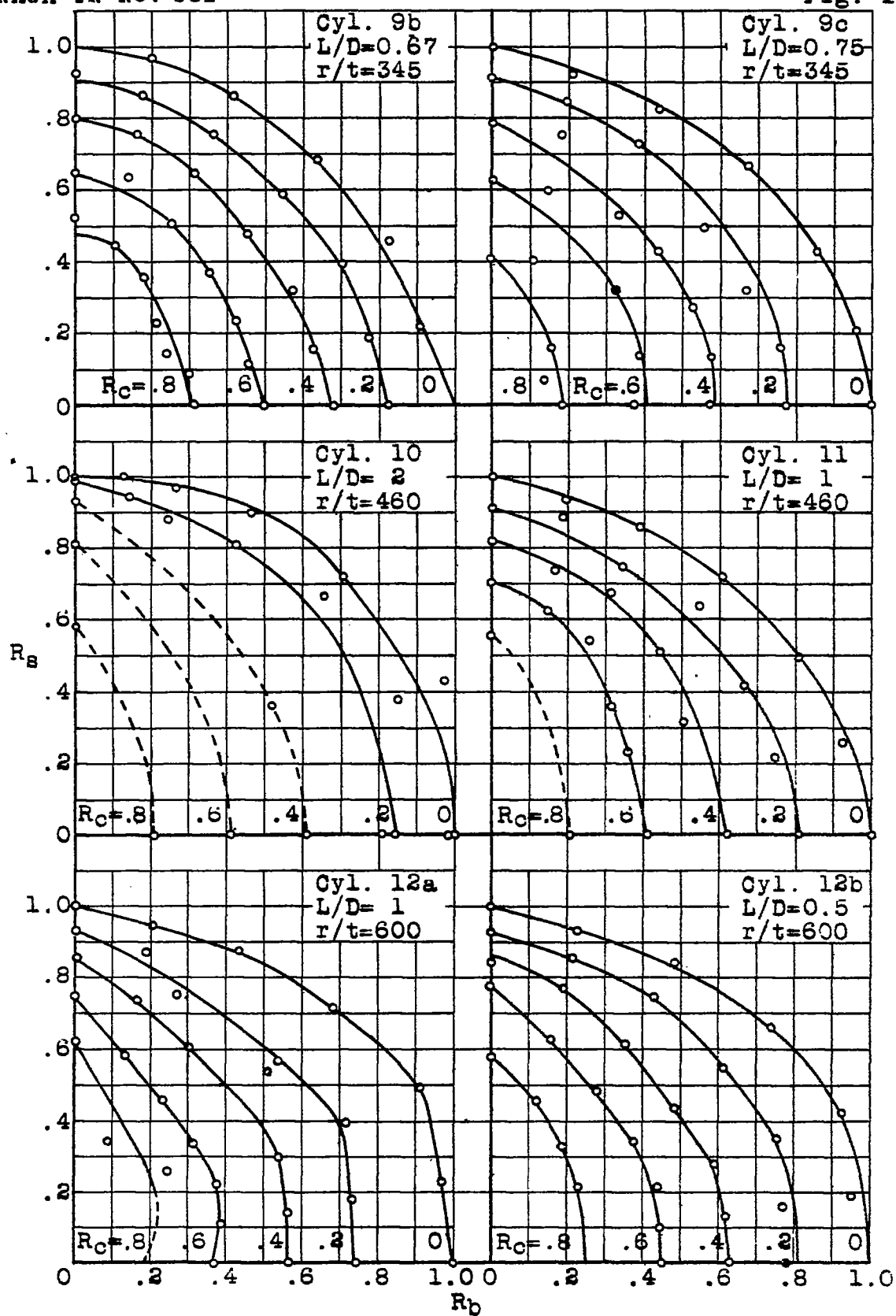
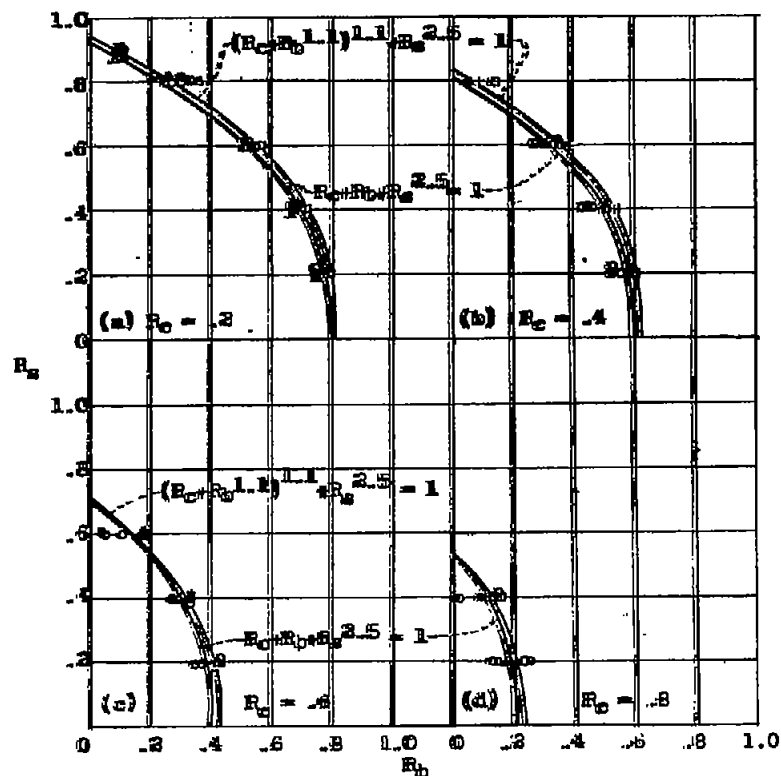


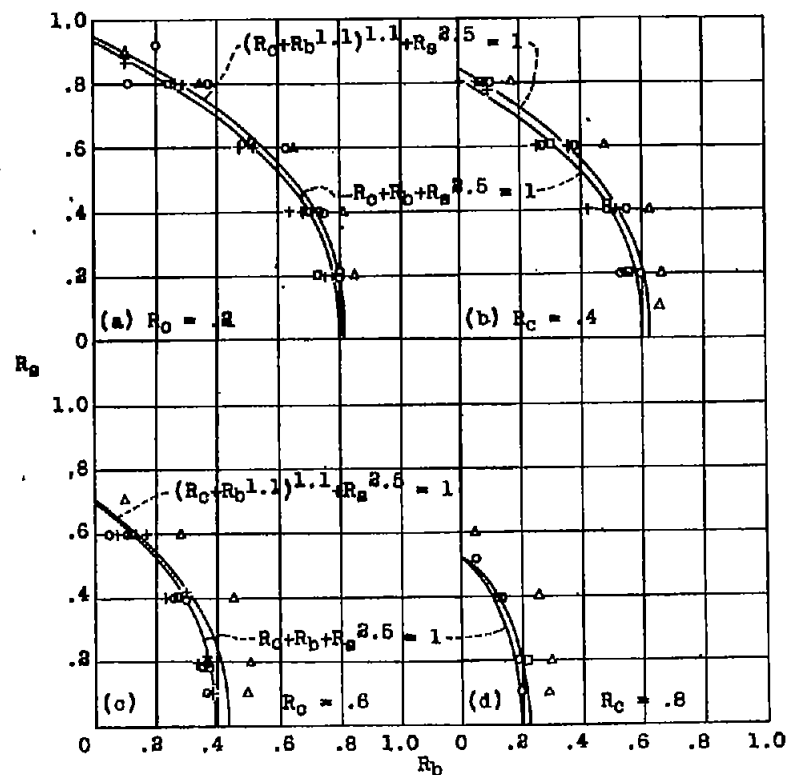
Figure 18.- Plot of test results for various test cylinders loaded in combined compression, pure bending and pure torsion.



Test data for test cylinders 2b, 3b, 7b, 8a, 9b, 9c, 12b.

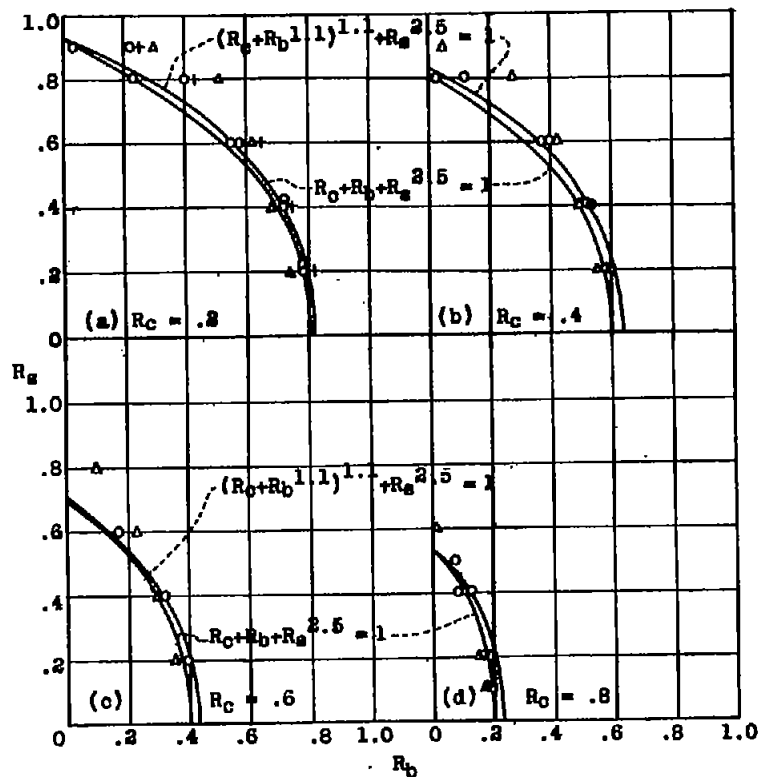
Figure 20.- Plot of test data for cylinders loaded in combined compression, pure bending and pure torsion. L/D ratio of cylinders = 0.5 approximately.

$r/t = 230 = \Delta$
 $r/t = 345 = \circ$
 $r/t = 460 = +$
 $r/t = 600 = \square$



Test data for test cylinders 1a, 1b, 2a, 3a, 11, 12a.

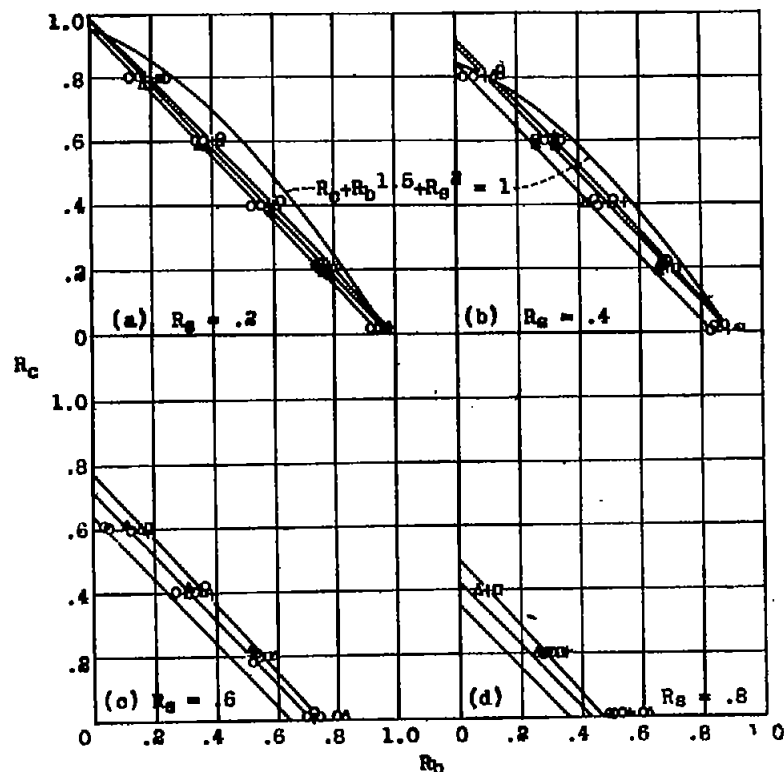
Figure 21.- Plot of test data for cylinders loaded in combined compression, pure bending and pure torsion. L/D ratio of cylinders = 1.0 approximately.



$r/t = 230 = \Delta$
 $r/t = 345 = \circ$
 $r/t = 480 = +$

Test data for test cylinders 5c, 7a, 9a, 10.

Figure 22.- Plot of test data for cylinders loaded in combined compression, pure bending and pure torsion. L/D ratio of cylinders = 2.0 approximately.



$r/t = 230 = \Delta$
 $r/t = 345 = \circ$

$r/t = 480 = +$
 $r/t = 600 = \square$

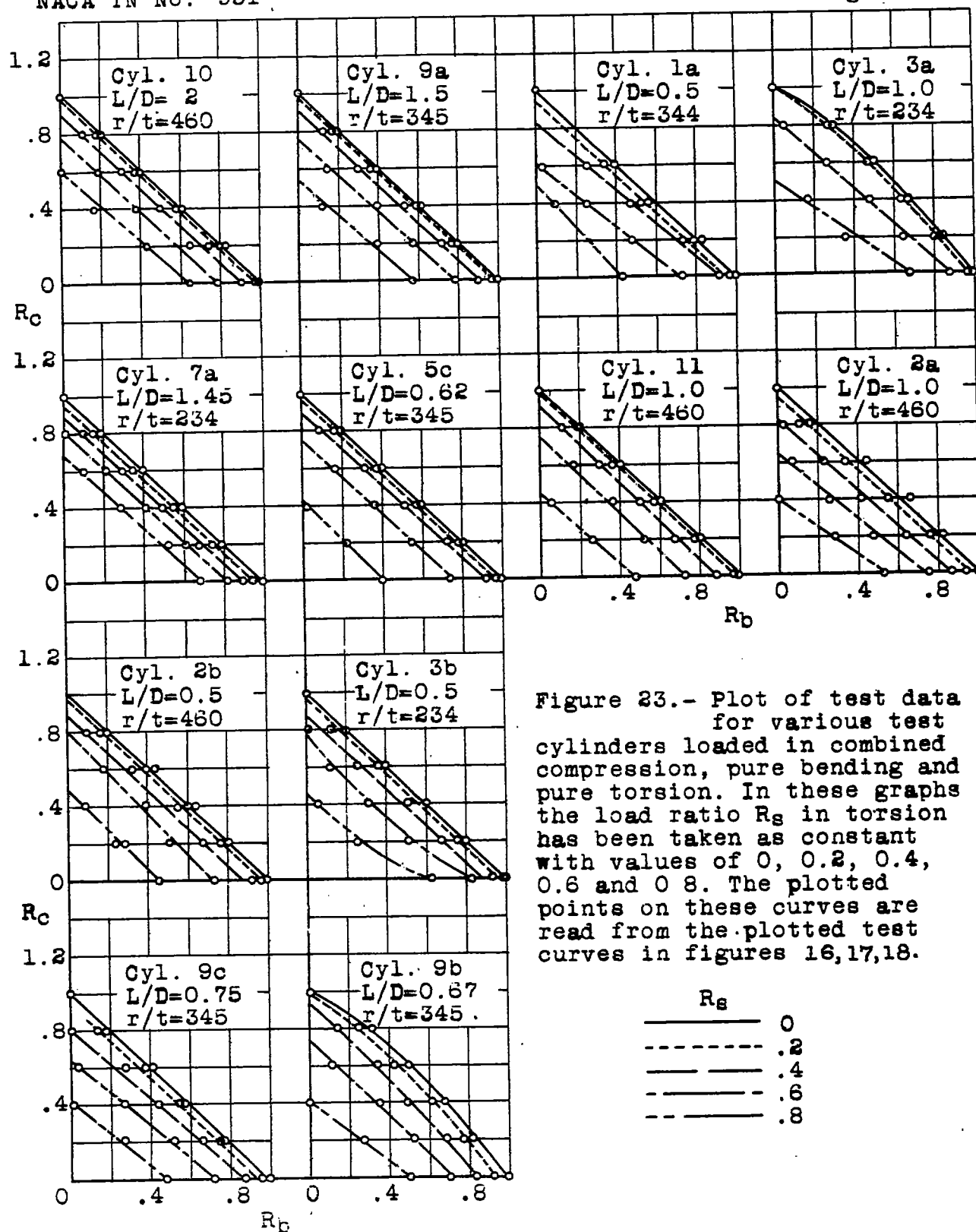
Explanation:

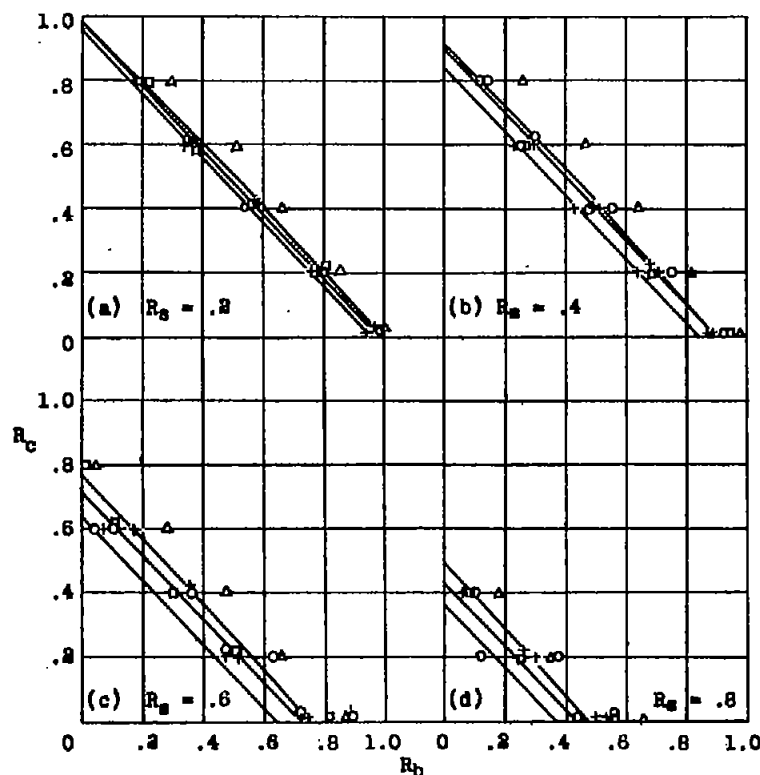
In the above results R_c is kept constant at the values shown and the corresponding values of $R_b + R_p$ were read from the curves representing the test data for the individual test cylinders as given in Figures 16, 17, and 18. For cylinder numbers plotted in this figure see information on Figure 20.

The diagonal lines as plotted represent the following interaction equations:

- upper line $(R_b + R_b^{1.1}) + R_c^{2.5} = 1$
- middle line $R_c + R_b + R_c^{2.5} = 1$
- lower line $R_c + R_b + R_c^2 = 1$

Figure 24.- Plot of test data for cylinders loaded in combined compression, pure bending and pure torsion. L/D ratio of cylinders = 0.5 approximately





$r/t = 330 = \Delta$
 $r/t = 345 = \circ$
 $r/t = 460 = +$
 $r/t = 600 = \square$

Explanation:

In the above results R_s is kept constant at the values shown and the corresponding values of $R_c + R_b$ were read from the curves representing the test data for the individual test cylinders as given in Figures 16, 17, and 18. The diagonal lines as plotted represent the following interaction equations:

upper line $(R_c + R_b)^{1.1} + R_s^{2.5} = 1$

middle line $R_c + R_b + R_s^{2.5} = 1$

lower line $R_c + R_b + R_s^2 = 1$

Figure 25.- Plot of test data for cylinders loaded in combined compression, pure bending and pure torsion. L/D ratio of cylinders = 1.0 approximately.

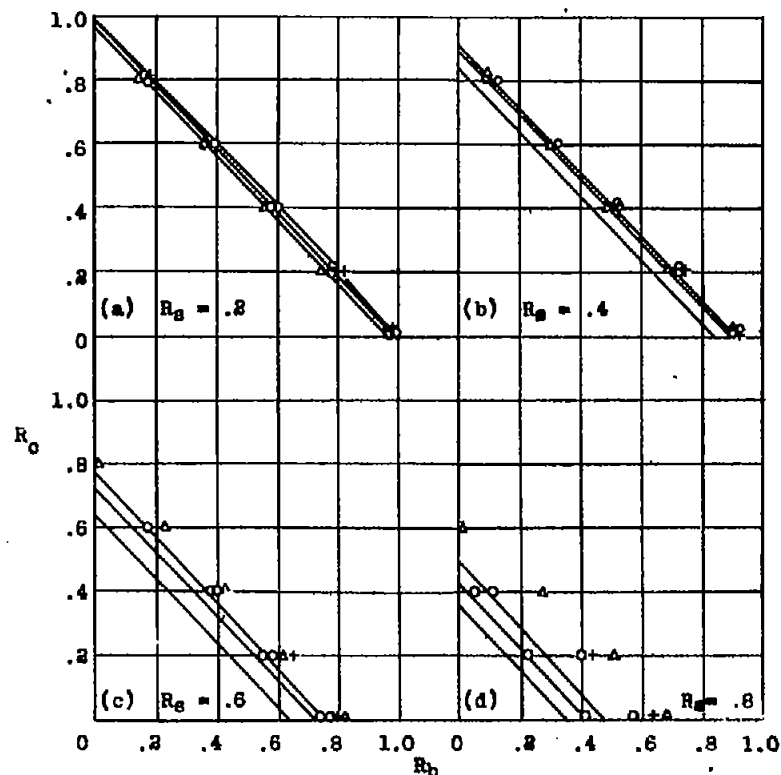
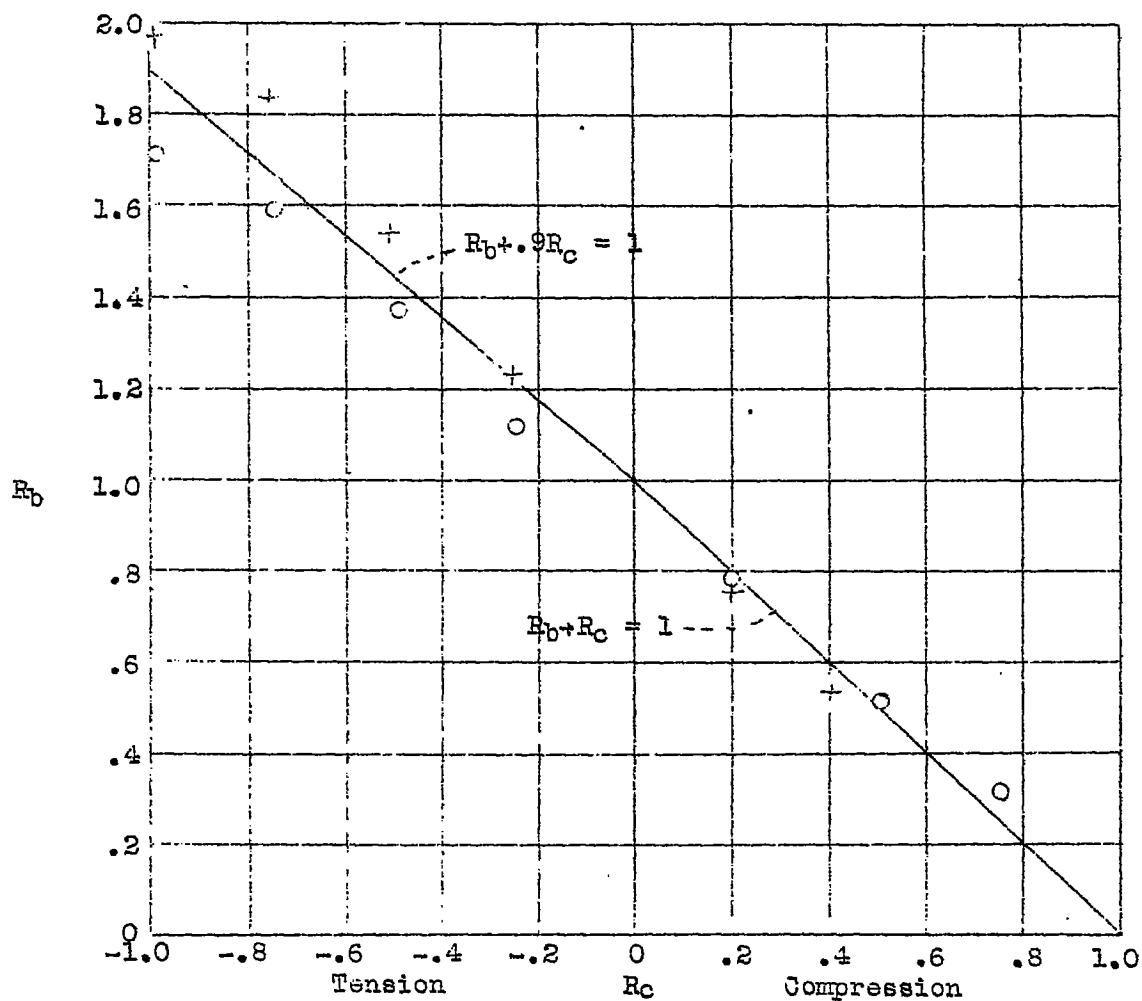


Figure 26.- Plot of test data for cylinders loaded in combined compression, pure bending and pure torsion. L/D ratio of cylinders = 2.0 approximately.



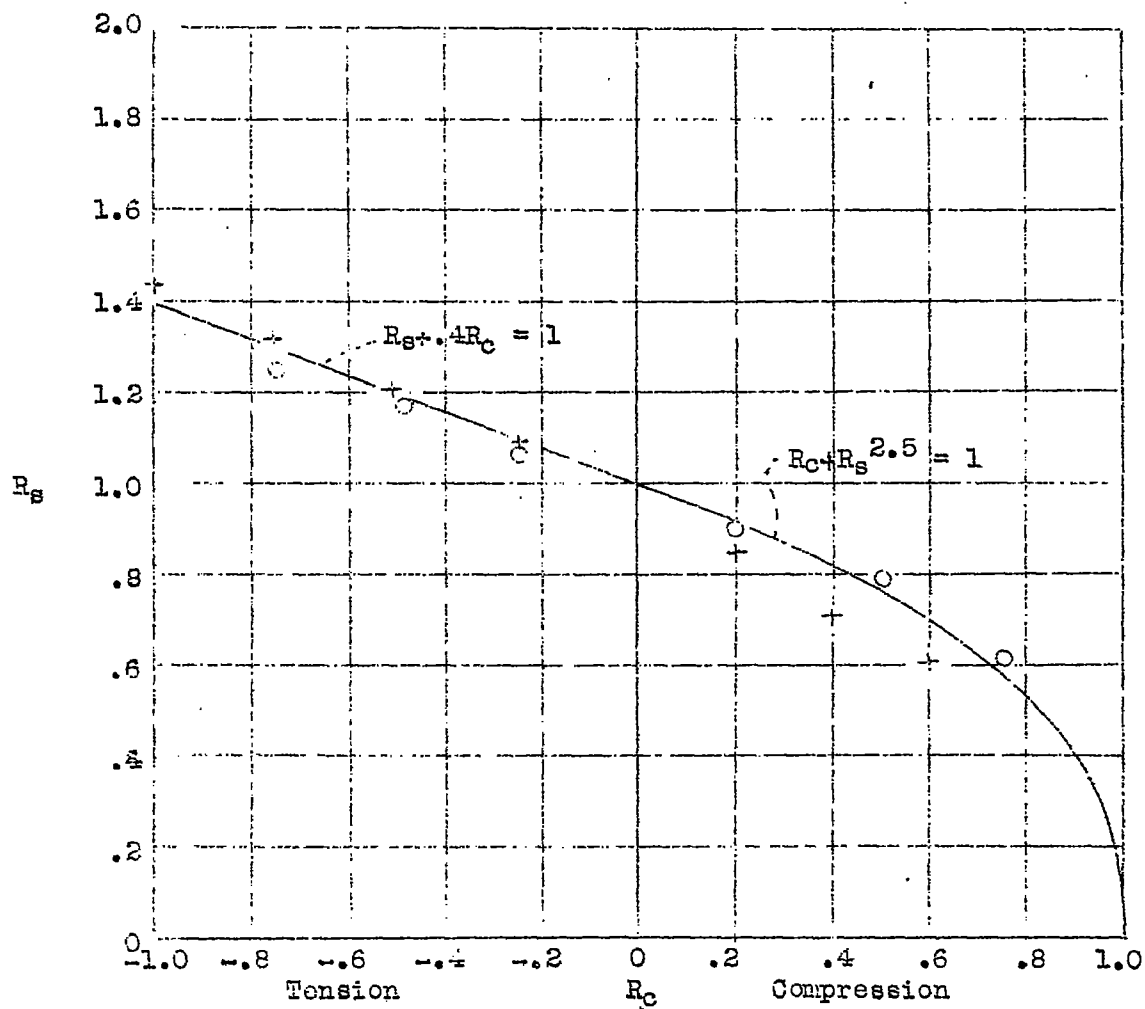
○ = test data for test
cylinder No. 13a

$L = 12''$
 $D = 12''$
 $t = .0075''$
 $L/D = 1$
 $r/t = 800$

+ = test data for test
cylinder No. 13b

$L = 6''$
 $D = 12''$
 $t = .0075''$
 $L/D = 0.5$
 $r/t = 800$

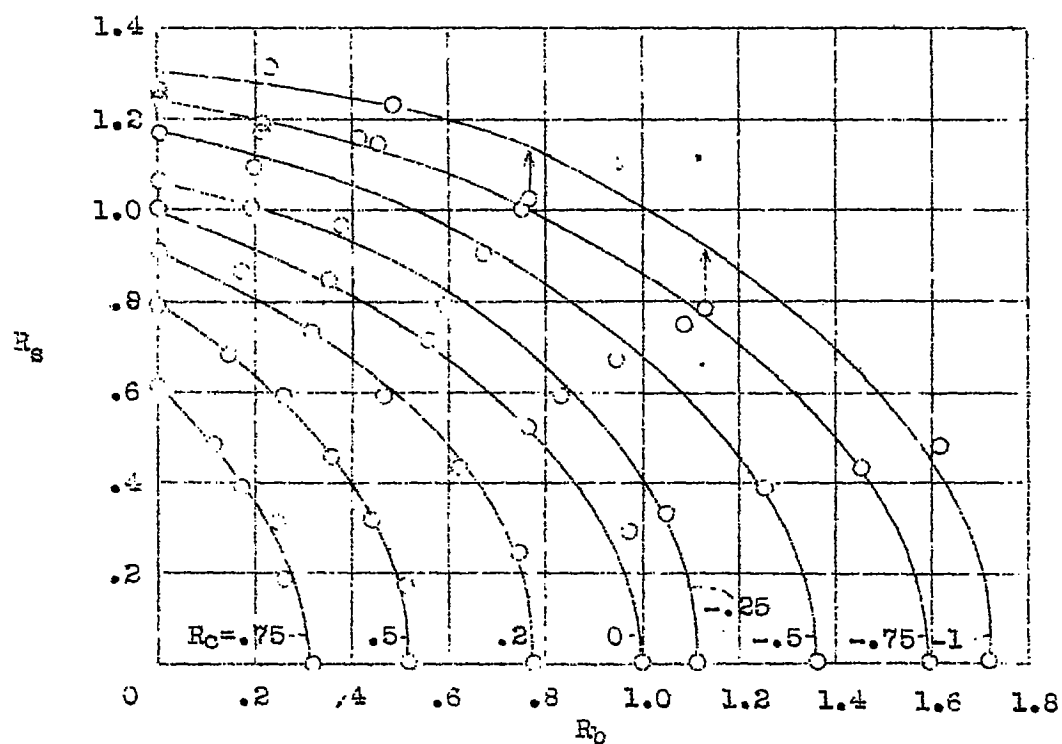
Figure 27.- Plot of test results for cylinders in tension or compression combined with pure bending.



○ = test data for test
cylinder No. 13a
 $L = 12''$
 $D = 12''$
 $t = .0075''$
 $L/D = 1$
 $r/t = 800$

+ = test data for test
cylinder No. 13b
 $L = 6''$
 $D = 12''$
 $t = .0075''$
 $L/D = 0.5$
 $r/t = 800$

Figure 28.- Plot of test results for cylinders in tension or compression combined with pure torsion.



Test results for cylinder No. 13a

$L = 12''$

$D = 12''$

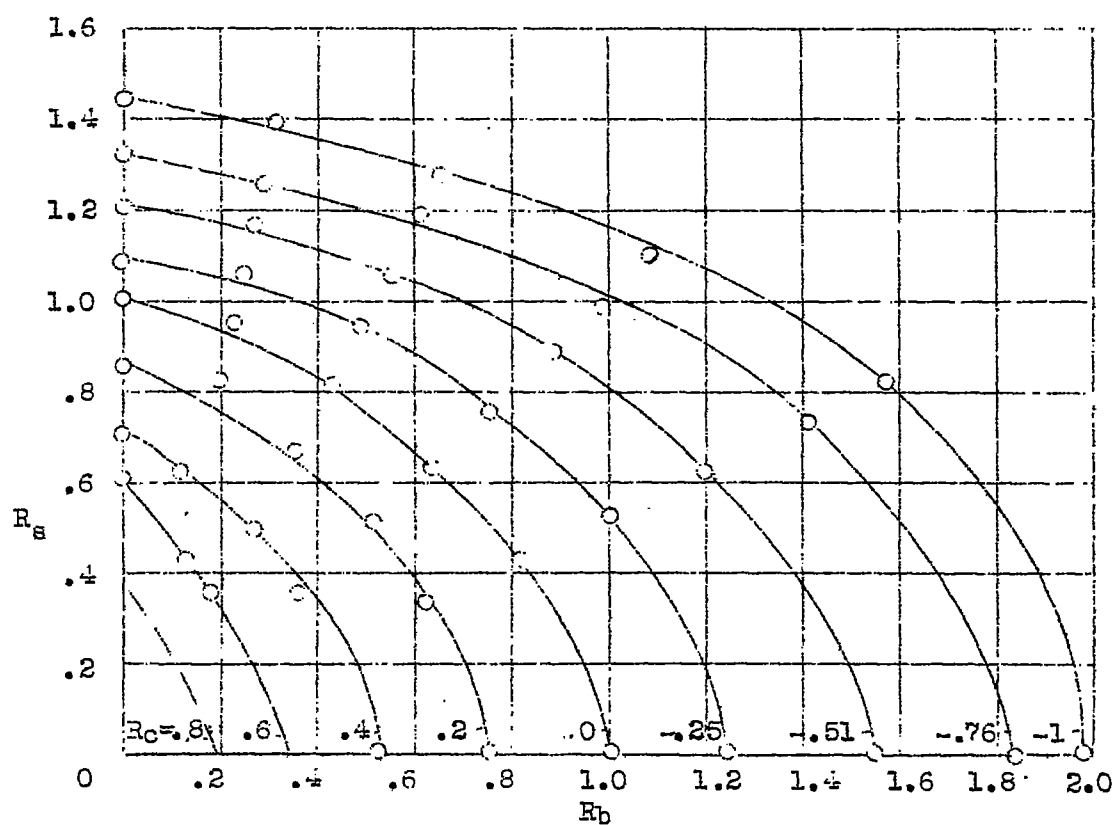
$t = .0075''$

$L/D = 1.$

$r/t = 800$

Note: minus sign for R_c represents tension load.

Figure 29.— Plot of test results for cylinders in tension or compression combined with pure bending and pure torsion.

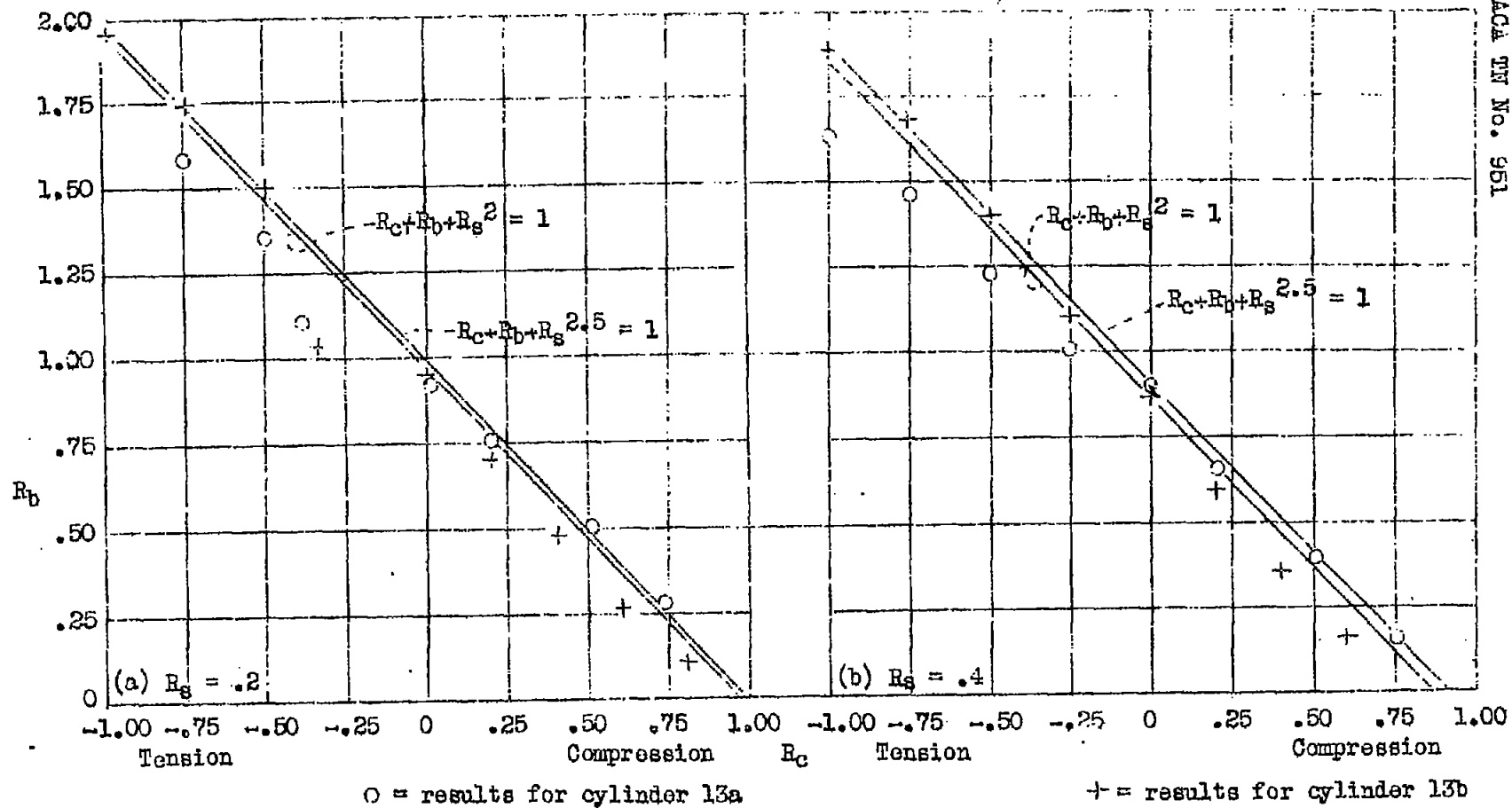


Test results for cylinder No. 13b

$L = 6''$
 $D = 12''$
 $t = .0075''$
 $L/D = 0.5$
 $r/t = 800$

Note: minus R_c represents tension load.

Figure 30.- Plot of test results for cylinder in tension or compression combined with pure bending and pure torsion.



(Torsion load ratio R_s kept constant at .2 and .4)

Figure 31.- Plot of test results for cylinders in combined tension, bending, and torsion.

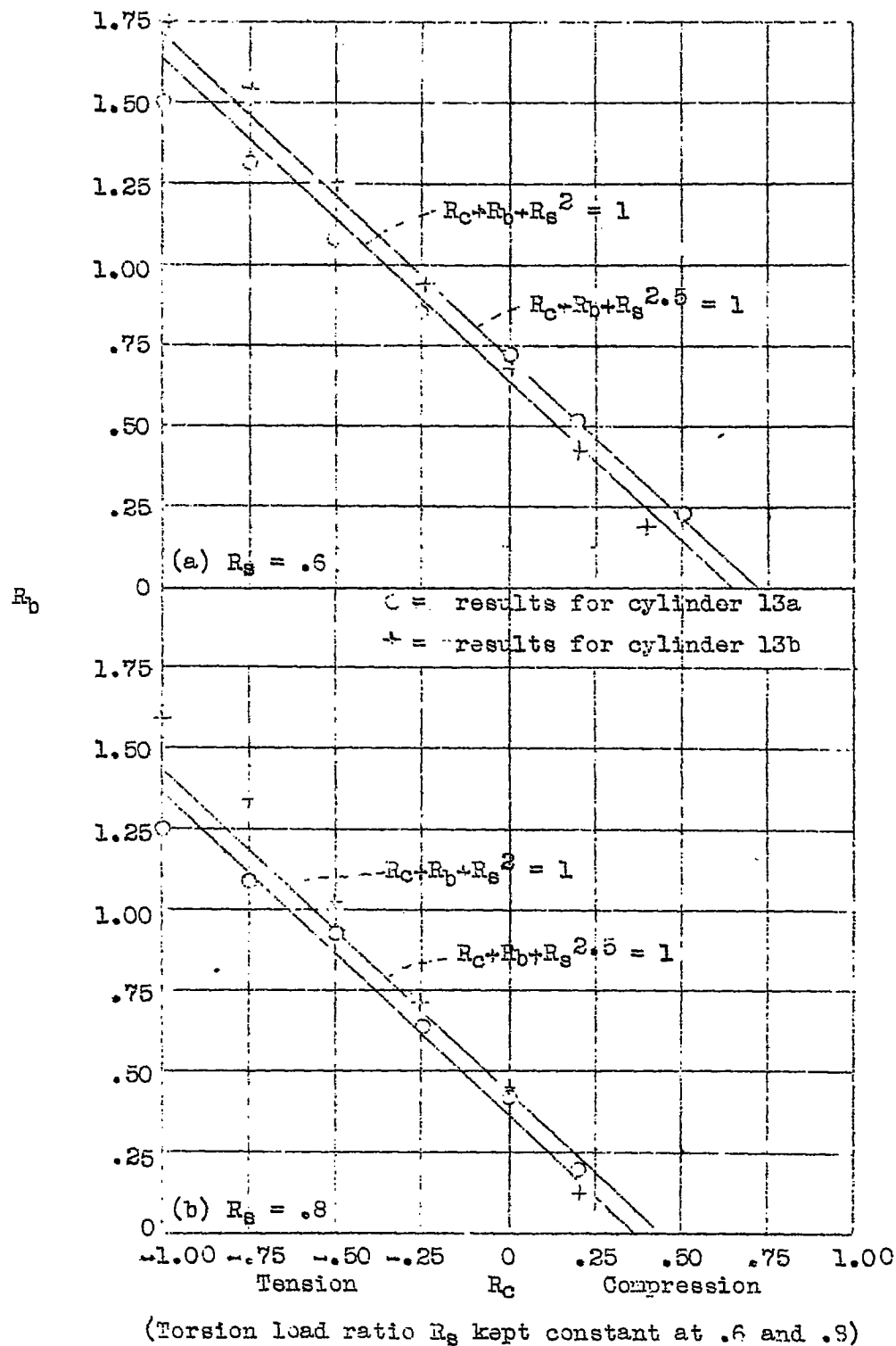


Figure 32.- Plot of test results for cylinders in combined tension, bending, and torsion.

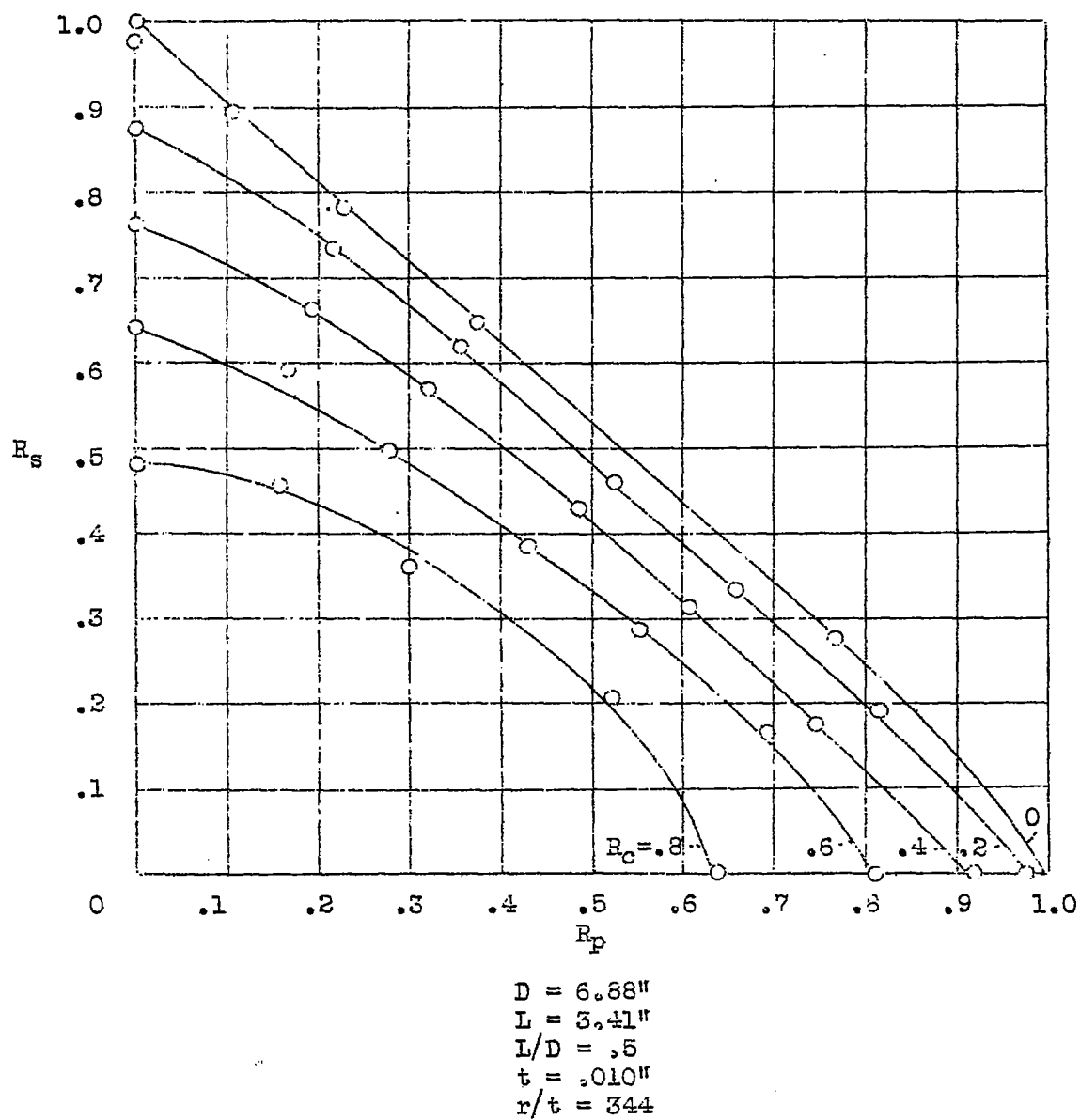


Figure 33.-- Test results for cylinder 6b when subjected to combined lateral bending, compression and pure torsion.

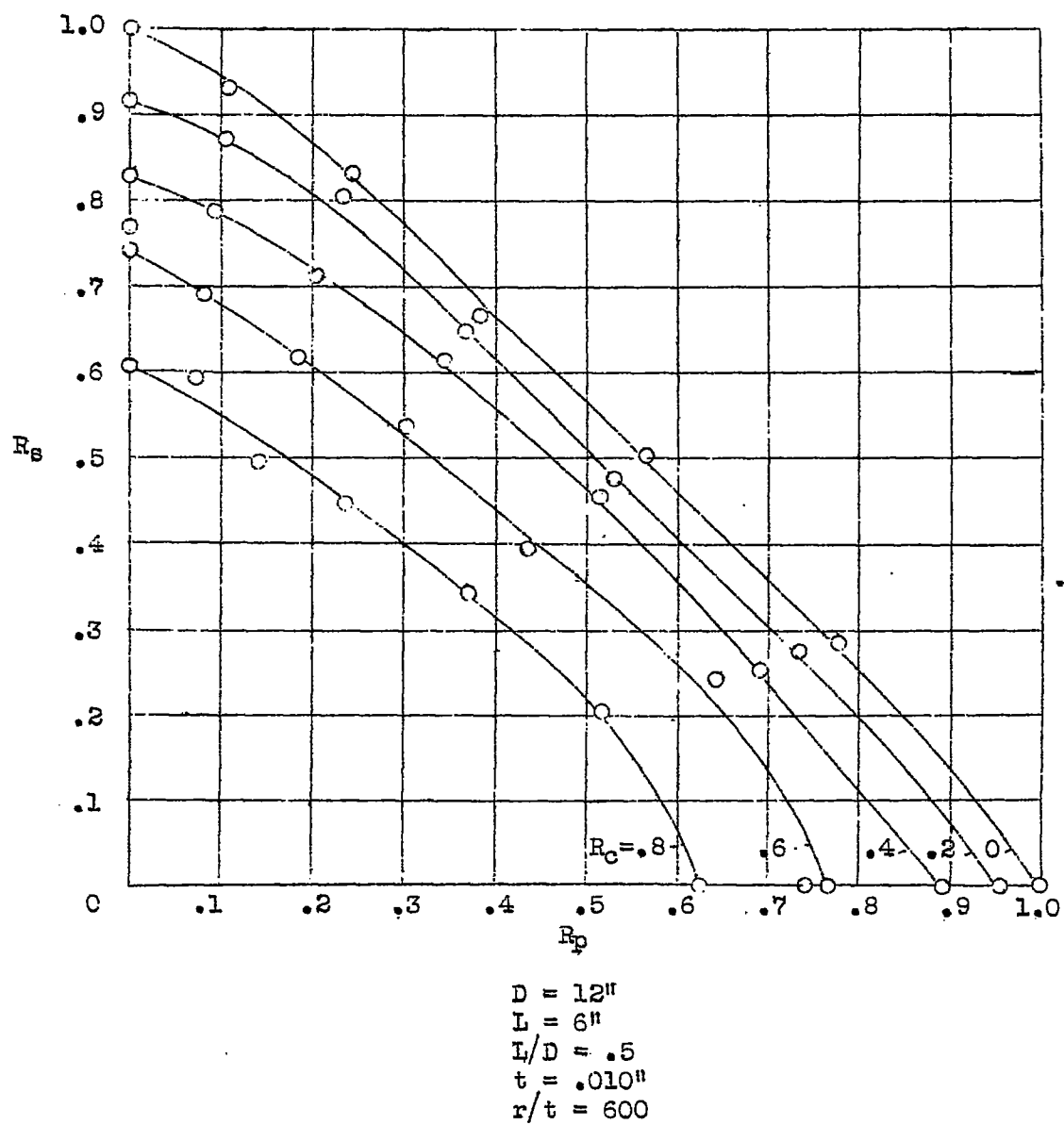


Figure 34.- Test results for cylinder 15 when subjected to combined lateral bending, compression and torsion.



Photo. No. 7. Failure of cylinder P-2 in pure bending. $L/D = 4$

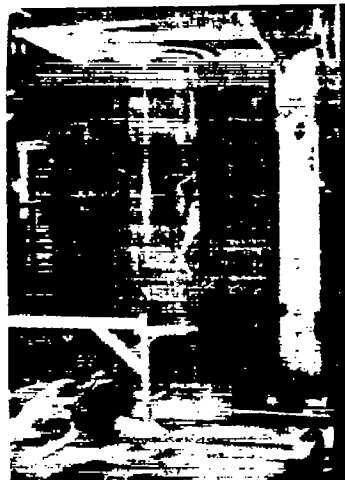


Photo. No. 8. Failure of cylinder P-2 in pure bending. Two intermediate bulkheads. $L/D = 2$

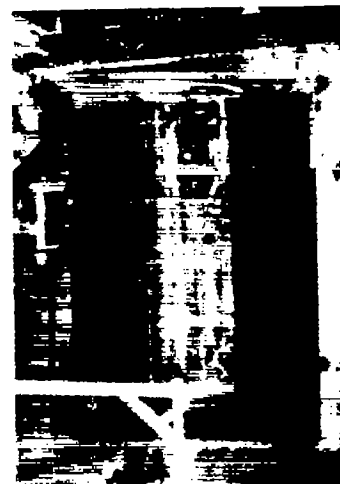


Photo. No. 9. Failure of cylinder P-2 in pure bending. Three intermediate bulkheads. $L/D = 1$



Photo. No. 4. Failure of cylinder P-2 in pure torsion. $L/D = 4$



Photo. No. 5. Failure of cylinder P-2 in pure torsion. Two intermediate bulkheads. $L/D = 2$



Photo. No. 6. Failure of cylinder P-2 in pure torsion. Three intermediate bulkheads. $L/D = 1$

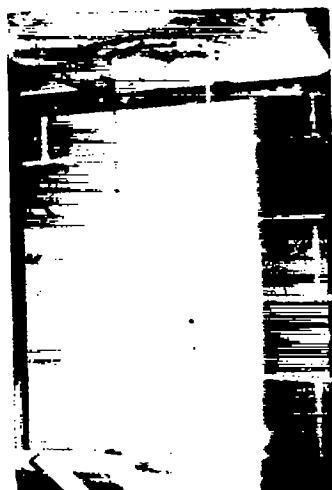


Photo. No. 3. Test cylinder P-2. $D = 7''$, $L = 23''$, $t = .010''$



Photo. No. 2. Test jig with 7" dia., 23" length cylinder in place.



Photo. No. 1. Operator measuring strain for determination of E .

Photographs of Tests on Preliminary Test Cylinder P-2. The chief purpose of these tests was to determine the influence of time rate of loading upon the bending and torsional strength and also the effect of repeated buckling failure upon the original buckling strength in pure bending and torsion.



Photo.No.17. The Complete Test Jig.
 1 - test cylinder
 2 - Lever arms for applying bending & torsion
 3 - Speed reducer for applying loads above
 4 - Lever arms for the compression linkage
 5 - Speed reducer for d.
 6 - Thermometer



Photo.No.10. Forms, Sample Cylinder and Bottom Bulkhead. A cylinder is being fabricated on the 7" dia. form, the sheet being held in place by cloth tape.

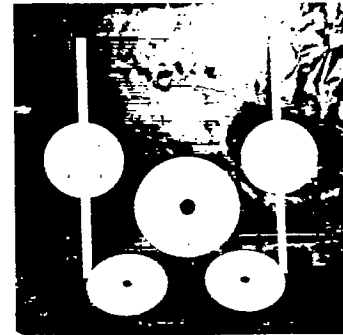


Photo.No.11. The upper bulkhead, two bottom bulkheads and two internal bulkheads for the 7" diameter test cylinders.



Photo.No.18. Operator Applying Loads to Test Cylinder.

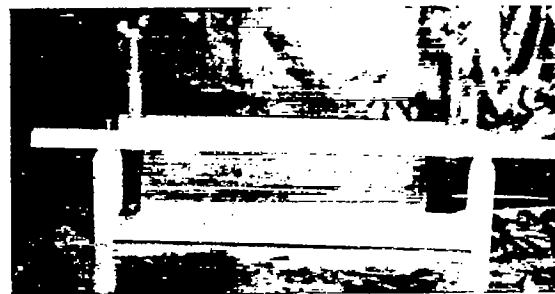


Photo.No.12. Jig for fabricating 12" diameter cylinders.

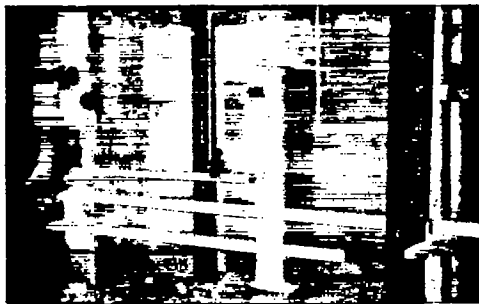


Photo.No.19. Photograph of 7" diameter cylinder buckling under combined pure bending and torsional loads.



Photo.No.13. A 12" diameter cylinder with end bulkheads ready for mounting in test jig.



Photo.No.14. A 7" diameter cylinder (L/D = 2) ready for mounting in test jig.



Photo.No.20. A 7" dia. 14" length cylinder with two internal bulkheads mounted in test jig.

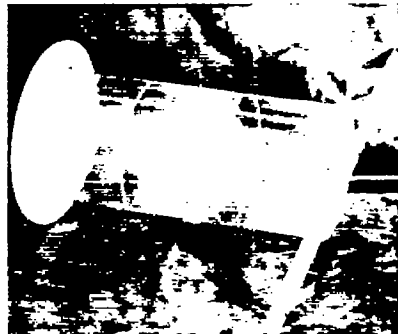


Photo.No.15. Same as cylinder in No.14 but with one internal bulkhead in position.



Photo.No.16. Same as cylinder in No.14 but with two internal bulkheads located at the third points.

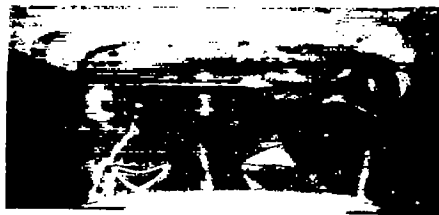


Photo.No.21. 12" cylinder buckling under pure compression load. $L/D = 0.5$

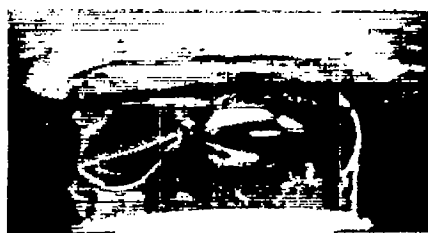


Photo.No.22. 12" cylinder buckling under pure bending load. $L/D = 0.5$



Photo.No.23. 12" cylinder buckling under pure torsion load. $L/D = 0.5$



Photo.No.24. 12" cylinder buckling under pure compression load. $L/D = 1$



Photo.No.25. 12" cylinder buckling under pure bending load. $L/D = 1$



Photo. No.26. 12" cylinder buckling under pure torsion load. $L/D = 1$



Photo.No.27. A 12" cylinder buckling under combined bending and compression loading. $L/D = 1$



Photo.No.28. A 12" cylinder buckling under combined compression and torsion load. $L/D = 1$



Photo.No.29. A 12" cylinder buckling under combined bending and torsion load. $L/D = 1$



Photo.No.33. Buckling of 7" cylinder in pure torsion. One internal bulkhead. $L/D = 2$

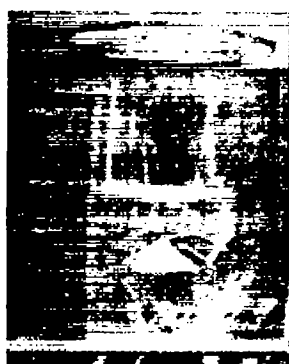


Photo.No.32. Buckling of 7" cylinder in pure bending. One internal bulkhead. $L/D = 2$



Photo.No.31. Buckling of 7" cylinder in pure compression. One internal bulkhead. $L/D = 2$

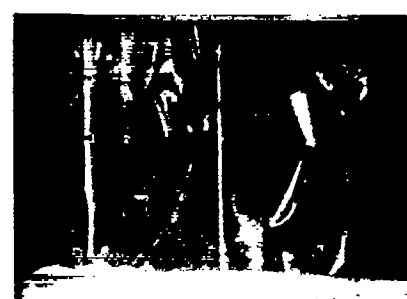


Photo No.30. A 12" cylinder buckling under a combined compression, bending and torsion load. $L/D = 1$

The magnitude of the buckles and wrinkles shown in the above photographs is greater than that permitted in the official cylinder tests since excessive buckling would tend to produce local weakness for repeated tests.